

ETHANOL MODULATION OF NMDA RECEPTORS AND
NMDAR-DEPENDENT LONG-TERM DEPRESSION IN THE DEVELOPING
JUVENILE DENTATE GYRUS

by

Scott D. Sawchuk

Bachelor of Science (Honours), University of Victoria 2015

A thesis submitted in partial fulfillment
of the requirements for the degree of

MASTER OF SCIENCE

in

The Division of Medical Sciences

Copyright © SCOTT D. SAWCHUK 2019

ALL RIGHTS RESERVED.

THIS THESIS MAY NOT BE REPRODUCED IN WHOLE OR IN PART, BY
PHOTOCOPYING OR OTHER MEANS, WITHOUT THE PERMISSION OF THE AUTHOR.

ETHANOL MODULATION OF NMDA RECEPTORS AND
NMDAR-DEPENDENT LONG-TERM DEPRESSION IN THE DEVELOPING
JUVENILE DENTATE GYRUS

by

Scott D. Sawchuk

Bachelor of Science (Honours), University of Victoria 2015

Supervisory Committee

Dr. Brian Christie, Division of Medical Sciences
Supervisor

Dr. Raad Nashmi, Department of Biology
Outside Member

Dr. Pedro Grandes, Division of Medical Sciences
Committee Member

Abstract

Long-term depression (LTD) induced by low frequency stimulation (LFS; 900x1Hz) at medial perforant path (MPP) synapses in the rat dentate gyrus (DG) has been described as both developmentally regulated and N-methyl D-aspartate receptor (NMDAr) independent, yet sufficient evidence suggest that the processes is not entirely independent of NMDAr activity. In the present study, *in vitro* DG-LTD_{LFS} was induced in hippocampal slices prepared from rats at postnatal day (PND) 14, 21 and 28 to investigate how the sensitivity of DG-LTD~LFS to the NMDAr antagonist amino-5-phosphonovaleric acid (AP5; 50 μ M) changes throughout the juvenile developmental period (jDP; PNDs 12-29) that occurs immediately after the period of peak neurogenesis. We further examined the acute effects of the partial NMDAr antagonist ethanol (EtOH) on DG-LTD_{LFS} and NMDAr excitatory post synaptic currents (NMDAr-EPSCs) in dentate granule cells (DGCs) using 50 and 100mM concentrations (50mM ~0.2%BAC) of EtOH.

The magnitude of LTD induced at all three time points was not statistically different between age groups, but the probability of successfully inducing LTD did decrease with age. We found that AP5 was insufficient to inhibit DG-LTD_{LFS} at PND14, but significantly inhibited DG-LTD_{LFS} at PND21 and PND28. We also found that 50mM EtOH, but not 100mM EtOH, significantly attenuated the magnitude of DG-LTD_{LFS} induced at each time point. Acute effects of 50mM EtOH had relatively little effect on NMDAr-EPSCs at PND14, and showed a slight potentiation of the response at PND21. 50mM EtOH at PND28, and 100mM EtOH at all three developmental time points showed inhibition of the NMDAr-EPSC. These findings provide insight on how developmental changes to the DG network and dentate granule cells (DGCs) influences mechanisms and processes involved in the induction and expression of synaptic plasticity in the DG.

Contents

Supervisory Committee	ii
Abstract	iii
Table of Contents	iv
List of Figures	v
List of Tables	vi
Acronyms	vii
Acknowledgments	viii
1 Introduction	1
Overview and Objectives	1
Experimental justification and hypotheses	6
Memory and the Hippocampus	7
Synaptic Plasticity	10
The N-methyl D-aspartate Receptor	14
The acute effects of Ethanol on the NMDAr and LTD	17
Ethanol on the NMDAr	17
Ethanol and LTD	18
The Dentate Gyrus	19
Anatomy & Development	19
Dentate Granule Cells	23
Long-Term Depression in the DG	26
Neurophysiology in the DG	28
2 Materials and Methods	31
Subjects:	31
Tissue Preparation:	31
Extracellular field electrophysiology:	33
Analysis of fEPSP slope	34
Whole-cell patch clamp electrophysiology:	35
Drugs	37
Statistics	37
3 Results	38
No significant change in the magnitude of DG-LTD _{LFS} between PND 14, 21, and 28.	38
AP5 inhibits DG-LTD _{LFS} at PND21 and PND28, but not at PND14	41
50mM EtOH attenuates DG-LTD _{LFS} at all points in the jDP	43
100mM EtOH has no significant effect on DG-LTD _{LFS} at any point through- out the jDP period	45

Acute 50mM EtOH has developmentally regulated effects on NMDAr-EPSCs	49
100mM EtOH trends towards inhibition at each time point	49
4 Discussion	53
Summary of results	53
DG-LTD _{LFS} throughout the jDP	54
No significant differences in the magnitude of LTD observed at PND14, PND21 and PND28	54
AP5 inhibits DG-LTD _{LFS} at PND21 & PND28, but not PND14	55
Deciphering the role of NMDARs in DG-LTD _{LFS}	56
Changes to NMDAr subunit expression throughout development may affect DG-LTD _{LFS} in the jDP	59
Conclusions and future directions regarding the role of NMDARs in DG-LTD	60
Effects of EtOH on NMDARs and DG-LTD _{LFS}	62
Developmental time point and concentration are both important factors to consider.	62
Deciphering the acute effects of EtOH on DG-LTD _{LFS} and NMDAr- EPSCs	64
Conclusions and future directions regarding the acute effects of EtOH on DGCs and DG-LTD _{LFS}	66
5 References	68

List of Figures

Figure	Page
1.1 Trisynaptic circuit	9
1.2 The NMDA receptor	16
1.3 Cells of the DG	21
1.4 DGC morphology	24
1.5 Experimental neurophysiology in the DG	30
3.1 DG-LTD LTD throughout the jDP	40
3.2 The effects of AP5 on DG-LTD LTD	42
3.3 The effects of 50mM EtOH on DG-LTD LFS	44
3.4 The effects of 100mM EtOH on DG-LTD LFS	46
3.5 Summary of DG-LTD LFS throughout the jDP	47
3.6 The effects of 50mM EtOH on NMDAr-EPSCs	51
3.7 The effects of 100mM EtOH on NMDAr-EPSCs	52

List of Tables

Table	Page
3.1 Summary of DG-LTD LFS and fEPSP characteristics	48

aCSF	Artificial cerebral spinal fluid
AP5	amino-5-phosphonovaleric acid
AMPAr	α -amino-3-hydroxy-5-methyl-4-isoxazolepropionic acid receptor
CA	cornu ammonis
CB1	Cannabinoid receptor 1
CNS	Central nervous system
EC	Entorhinal cortex
EPSP	Excitatory post-synaptic potential
ExPSP	Experimental post-synaptic potential
fEPSP	Field excitatory post-synaptic potentials
DG	Dentate gyrus
DG-LTD	Dentate gyrus long-term depression
DG-LTD _{LFS}	Low frequency stimulation induced dentate gyrus long-term depression
DG-LTD _{Chem}	Agonist induced long-term depression
DGC	Dentate granule cell
GABA A	γ -aminobutyric acid receptor A
GCL	Granule cell layer
Hz	Hertz
jDP	Juvenile developmental period
LFS	Low frequency stimulation
LTD	Long-term depression
LTP	Long-term potentiation
LEC	Lateral entorhinal cortex
MEC	Medial entorhinal cortex
mGluR	Metabotropic glutamate receptor
ML	Molecular layer
MPP	Medial perforant path
MTL	Medial temporal lobe
NMDAr	N-methyl d-aspartate receptor
PND	Postnatal day
PHc	Parahippocampal cortex
PRc	Perirhinal cortex
PTX	Picrotoxin
Sb	Subiculum
SC	Schaffer collateral
SGZ	Subgranular zone
TRPV	Transient receptor potential vanilloid receptor

ACKNOWLEDGEMENTS

A great many people went into making this possible.

I'd like to thank Dr. Christie for giving me the space to work, and the freedom to make mistakes.

I'd like to thank Dr. Nashmi for being there since the beginning, and Dr. Grandes for helping me see the end.

I'd like to thank the members of the Christie lab who helped me through, and those who volunteered their time to make my life easier.

I'd like to thank those who have spurred a great many conversations.

I'd like to thank my mother and father for teaching me, and letting me, always ask questions.

I'd like to thank my brother for always keeping me connected to the other side of things.

I'd like to thank Love for helping me better understand what is important.

Dedicated to my cat.

CHAPTER 1

Introduction

Overview and Objectives

The dentate gyrus (DG) is a substructure of the hippocampus important in learning and memory (Amaral and Witter 1989; Squire and Zola-Morgan 1991; Kesner 2018), and is an integral part of the hippocampal tri-synaptic circuit (Figure 1.1). The DG is populated by small ovoid shaped cells called dentate granule cells (DGCs) that differ greatly from the rest of the hippocampal pyramidal cells (Carnevale et al. 1997). In the rodent, the DG is often considered a late developing structure due to the fact that the primary period of peak neurogenesis occurs postnatally (PNDs 5-12) (Rahimi and Claiborne 2007). This makes the DG a particularly important region of the brain for examining developmental changes to cell and network physiology.

The study outlined in this master's thesis uses young rats (postnatal days (PNDs); 14, 21 and 28) to investigate how development affects the sensitivity of N-methyl d-Aspartate receptors (NMDARs) to ethanol (EtOH) at medial perforant path (MPP) synapses in the dentate molecular layer of the hippocampus throughout the juvenile developmental period (jDP). These time points were chosen to reflect the period of DG development in the weeks immediately following the postnatal period of peak neurogenesis (PNDs 5-12) (Bayer and Altman 1974; Rahimi and

Claiborne 2007).

I studied the involvement of NMDARs in DG long-term depression (LTD) induced by low-frequency stimulation (DG-LTD_{LFS}) at MPP-dentate granule cell (MPP-DGC) synapses, and investigated the impact of acute EtOH exposure (50 & 100mM) on DG-LTD_{LFS}. Furthermore, the sensitivity of evoked NMDAR excitatory post-synaptic currents (NMDAR-EPSCs) to acute EtOH exposure was examined at each developmental time point. I focused on these synapses for three major reasons. First, they integrate the hippocampal excitatory tri-synaptic circuit involved in learning and memory; second, MPP synapses show high efficiency in neuronal activation; and third, but not least, persistent EtOH intake damages the entorhinal corex (EC) and DG, impairing synaptic transmission and plasticity in this region.

LTD is a decrease in synaptic efficacy that is often induced *in vitro* by LFS (1-5Hz) over an extended period of time (5-15 minutes) (Dudek and Bear 1992; Collingridge et al. 2010; Pinar et al. 2017). This process is dependent on Ca²⁺ signaling (Mulkey and Malenka 1992; Harney, Rowan, and Anwyl 2006) and has been shown to involve simultaneous and distinct homosynaptic and heterosynaptic signaling mechanisms (Abraham et al. 1994; Debanne and Thompson 1996; Oliet, Malenka, and Nicoll 1997; Camodeca et al. 1999; Lisman 2017) in both the presynaptic and postsynaptic terminals (Castillo 2012). LTD in the DG has been shown to involve, but is not limited to, the NMDA receptor, mGluR receptors, voltage-gated Ca²⁺ channels, and endocannabinoid receptors (Desmond et al. 1991; Christie and Abraham 1992b; S. M. O'Mara, Rowan, and Anwyl 1995; Trommer, Liu, and Pasternak 1996; Chávez, Chiu, and Castillo 2010; Castillo 2012; Lovinger and

Abraham 2018). Developmental factors are proposed to be involved in the induction and expression of LTD (Trommer, Liu, and Pasternak 1996; Milner et al. 2004), and in the DG, the magnitude and probability of inducing LTD has been shown to decrease over the jDP (postnatal days (PNDs) 8-30) (Trommer, Liu, and Pasternak 1996). The role of NMDARs in DG-LTD remains controversial (Desmond et al. 1991; Christie and Abraham 1992a; S M O'Mara, Rowan, and Anwyl 1995; Wang, Rowan, and Anwyl 1997; Pöschel and Stanton 2007), but how the sensitivity of traditional LTD_{LFS} (900x1Hz) to inhibition of NMDARs changes throughout the jDP has not been explicitly shown. EtOH inhibition of NMDARs and synaptic plasticity *in vitro* is well documented (Lima-Landman and Albuquerque 1989; Lovinger, White, and Weight 1989; Hendricson et al. 2002; Izumi et al. 2005; Chandrasekar 2013; Zorumski, Mennerick, and Izumi 2014), but attention to field of study in the hippocampus has been almost exclusively in the *cornu ammonis* (CA) region, and almost entirely focused on long-term potentiation (LTP) over LTD. NMDAR are regularly reported to be inhibited by EtOH across a range of concentrations ([1:100 mM] EtOH; BAC of 50mM ~ 0.2%) (Wright, Peoples, and Weight 1996; Ariwodola et al. 2003; Mamei 2005), yet this inhibition remains incomplete at experimentally high concentrations ([100:500 mM] EtOH) (Wright, Peoples, and Weight 1996; Xu et al. 2012). Few reports exist that examine how EtOH modulates NMDAR-EPSCs in the DG (Ariwodola et al. 2003; Morrisett and Swartzwelder 1993), and to the best of our knowledge there are none on how acute EtOH impacts LTD in the juvenile rat DG.

Three main objectives are outlined in this work:

1. To better understand how changes to synaptic efficacy brought about by LFS (900x1Hz) in the developing juvenile DG varies as a function of developmental time point, and to gain a better understanding of how developmental time point may influence the role of NMDARs in DG-LTD_{LFS}. DG-LTD has been shown to be readily induced by the activation of mGluRs (S M O'Mara, Rowan, and Anwyl 1995; Wang, Rowan, and Anwyl 1997), and significant magnitudes of DG-LTD_{LFS} have been reported in the presence of the NMDAR inhibitor AP5 (Trommer, Liu, and Pasternak 1996; Wang, Rowan, and Anwyl 1997; Camodeca et al. 1999). For this reason the role of NMDAR in DG-LTD_{LFS} remains relatively unclear (Pöschel and Stanton 2007). How that role changes throughout the jDP has not been investigated.
2. To gain an understanding of how acute EtOH affects DG-LTD_{LFS}, and how this sensitivity changes throughout the jDP. 50 and 100mM concentrations of EtOH were chosen (50mM ~ 0.2BAC; Canadian legal limit: 0.05BAC) because these concentrations are physiologically attainable in humans and are regularly reported on in the literature. These effects were investigated at each developmental time point to determine if any effect on DG-LTD_{LFS} may change throughout the jDP. How EtOH affects LTD_{LFS} is not well understood (Hendricson et al. 2002; Izumi et al. 2005; Lovinger and Abrahao 2018), and to the best of my knowledge has not been examined in the DG. EtOH is a partial NMDAR antagonist (Lovinger, White, and Weight 1989; Lima-Landman and Albuquerque 1989; Wirkner et al. 1999) proposed to have differential effects on NMDARs based upon subunit composition (Zhao et al. 2015). The effects

of EtOH have been shown to be developmentally regulated with respect to glutamatergic and GABAergic neurotransmission (Mameli 2005; Fleming, Wilson, and Swartzwelder 2007), but how this translates to DG-LTD_{LFS} is currently unknown.

3. To contribute a study to the literature on the acute modulation of NMDAR-EPSCs by EtOH in the rat DG. This topic has received relatively little attention (Morrisett and Swartzwelder 1993; Ariwodola et al. 2003) compared to the CA1 (Lovinger, White, and Weight 1989; Lahnsteiner and Hermann 1995; Peoples et al. 1997; Puglia and Valenzuela 2010), and these effects have not been examined at distinct time points in the jDP. The DG undergoes significant changes to the NMDAR subunit expression profile during maturation (Coultrap et al. 2005), and each newborn DGCs undergoes a period of development with distinct changes to the NMDAR subunit populations being expressed (Ye et al. 2000; Liu et al. 2000). This makes the DG a mosaic of immature and mature cells, each expressing some variation of a developmentally regulated NMDAR subunit profile (Mu et al. 2015). The initial developmental period for DGCs is considered to occur over the first 14 days after cell differentiation, and further maturation of the dendritic tree and spine morphology has been described up until the cell reaches 60 days (Rihn and Claiborne 1990; Jones et al. 2003; Rahimi and Claiborne 2007). The majority of DGCs will still be relatively immature by the end of the second postnatal week (PND14), and will likely be affected by acute EtOH exposure in ways different than the more mature neurons of the late jDP.

Experimental justification and hypotheses

Reports have suggested the impact of EtOH on NMDARs differs between potential NMDAR subunit combinations (Ren et al. 2012; Zhao et al. 2015), and as the DG matures, NMDAR subunit expression changes drastically (Ye et al. 2000; Pedroni et al. 2014). Interestingly, acute EtOH exposure during LTD_{LFS} has been reported to both enhance (Hendricson et al. 2002) and inhibit (Izumi et al. 2005) the magnitude of LTD in the CA1. It is notable that these experiments were performed on rats either from the early jDP (PNDs 12-20) or the late jDP (PNDs 30-32) respectively. The effect of EtOH on LTD_{LFS} has not been shown in the DG, where the influence of development on acute sensitivity is an important factor to consider.

The few studies on how acute EtOH impacts NMDAR-EPSCs in the DG (Ariwodola et al. 2003; Morrisett and Swartzwelder 1993) have suggested inhibition similar to that seen in the CA1, where evidence supports developmental time point being an important factor in determining the acute sensitivity of EtOH to NMDARs (Mameli 2005). The majority of DGCs are born postnatally and undergo a developmental period lasting ~60 days that includes robust changes to NMDAR subunit expression. How the sensitivity of NMDAR-EPSCs to EtOH changes in the DG throughout the jDP has not been shown.

We sought to determine if postnatal time point during the weeks immediately following peak neurogenesis impacts the sensitivity of NMDAR-EPSCs and DG-LTD_{LFS} to acute exposure to 50 & 100mM EtOH concentrations. Because the role of NMDARs in DG-LTD_{LFS} is not well understood, and because EtOH is considered

a NMDAr antagonist, we also sought to determine if developmental time point impacts the sensitivity of DG-LDT_{LFS} to AP5. I hypothesize that maturation of the network architecture and changes to the NMDAr subunit profile impacts the sensitivity of DG-LTD_{LFS} to AP5 and EtOH in the developing juvenile rat DG. I further hypothesize that these changes also contribute to a developmental sensitivity of the acute effects of EtOH on NMDAr-EPSCs. We examine these questions using whole-cell patch clamp and field electrophysiology at PNDs 14, 21, and 28.

Memory and the Hippocampus

The hippocampus is part of the medial temporal lobe (MTL), which also includes the EC, and the perirhinal (PRc), and parahippocampal (PHc) cortices. The brain structures that make up the MTL system are critical for memory formation, retention and recall (Squire and Zola-Morgan 1991). The hippocampus was first implicated in the formation of new memories after a surgical lesion to the hippocampus of Henry Molaison, better known as patient H.M., resulted in severe anterograde amnesia characterized by the inability to form certain types of new memories (Scoville and Milner 1957; Squire 2009). The unfortunate case of Henry Molaison provided major insights into how the MTL contributes to memory formation, retention and recall. A major contribution of this work to the field of memory was in identifying the difference between declarative (explicit) and procedural (implicit) memory. Declarative memory is the type of memory allocated to remembering facts, including people, places and events, and is dependent on the hippocampus. Procedural memory on the other hand is evolutionarily older, and is important in the types of memory involved

in perceptual skills and motor tasks.

The hippocampus formation runs from the septal nuclei to the temporal cortex, mimicking the shape of banana. The long axis is referred to as the septotemporal axis and at 90 degrees to this is the transverse axis. A simplified version of hippocampal circuitry is often referred to as the tri-synaptic circuit (Figure 1.1). The tri-synaptic circuit describes the one-way flow of information through the hippocampus, beginning with input to the DG from the EC via the perforant pathway. The EC is uniquely placed as an interface between the neocortex and the hippocampal formation (Hafting et al. 2005). Like the rest of the cortex, comprises six layers compared to the 3 layers of the hippocampus and is subdivided into the medial and lateral entorhinal cortices (MEC & LEC). DG axons, called mossy fibers, project to pyramidal cells of the CA3 region and synapse in the proximal region of the apical CA3 dendritic field called the stratum lucidum, and CA3 axons project along the schaffer collateral (SC) pathway to the pyramidal cells of the CA1. The CA3-CA1 SC pathway is one of the most well studied pathways in the brain, as it exhibits a number of plastic processes that are relatively easily studied. Axons leaving the CA1 project to the subiculum (Sb) before returning to the EC (Amaral and Witter 1989), completing the circuit. This simplified version of information flow through the hippocampus has been important in gaining an understanding of principles of neural circuitry, and has been highly influential in developing models of synaptic plasticity that can be translated into theories of learning & memory.

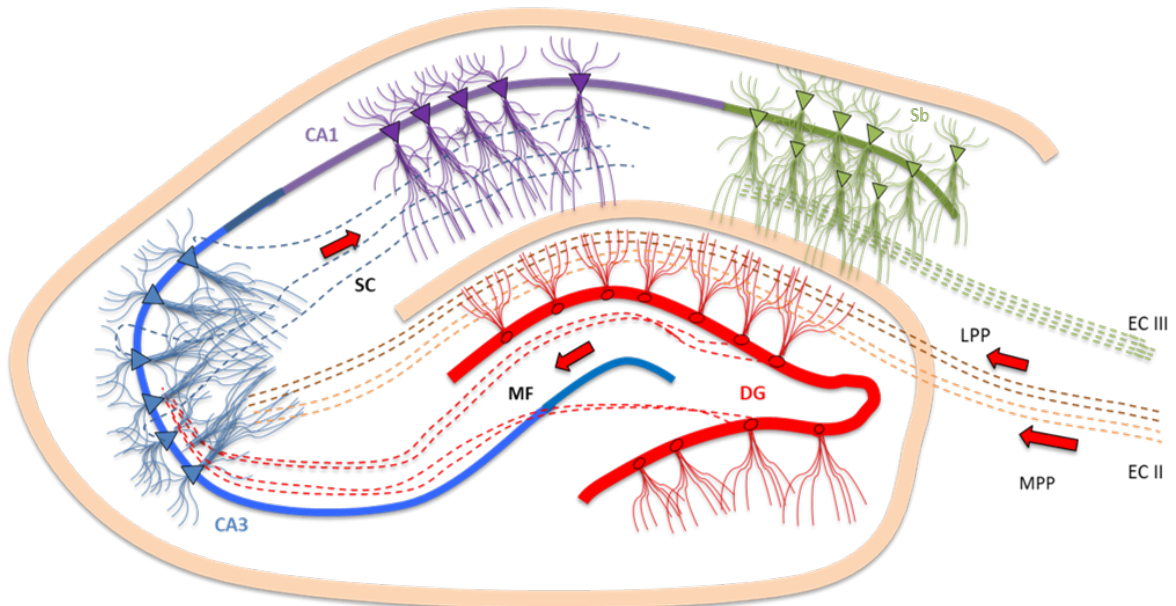


Figure 1.1: The hippocampal trisynaptic circuit describes the basic flow of information through the hippocampus. The principle excitatory input to the hippocampus originates in the EC via PP axons that form *en passant* synapses with DGCs of the DG before terminating in the distal dendritic field of the CA3. Excitation of DGCs sends information along the MF pathway to the CA3, where information input processed by the DG is integrated into the CA3 network. Sufficient excitation of CA3 pyramidal cells sends information along the SC pathway, connecting the CA3 to the CA1. Information then passes between the CA1 and the Sb before leaving the HC back to the EC. **Abbreviations:** *Cornu ammonis* regions (CA3, CA1); Dentate gyrus (DG); Entorhinal cortex (EC); Lateral perforant path (LPP); Medial perforant path (MPP); Mossy fibers (MF); Schaffer collaterals (SC); Subiculum (Sb)

Synaptic Plasticity

Synaptic plasticity refers to changes to neurotransmission induced and expressed in response to electrical and chemical signalling between brain cells. The concept of learning being associated with changes to synaptic communication was initially proposed by Santiago Ramón y Cajal (Cajal 1894) based on observations from his anatomical work. The principle theory was greatly expanded upon by Donald O. Hebb (1949), who theorized how neuronal communication could change given sufficient input. Manipulating observable phenomenon like habituation, sensitization and desensitization in the gill withdrawal reflex in *Aplysia* (Kandel and Spencer 1968) provided significant insight to how the field of synaptic plasticity could relate to behavioral changes. Early investigations to inducible changes in synaptic efficacy showed adaptations in responses that were relatively short lived, and long-term changes to synaptic efficacy became a distinguished field of study after long-term synaptic potentiation was shown in the DG of the anesthetized rabbit (Bliss and Gardner-Medwin 1973).

Mechanisms involved in the induction and expression of synaptic plasticity can be first described by their location and persistence (Lisman 2017). Synaptic plasticity can be expressed in both the pre-synaptic and post-synaptic terminals (Rollenhagen et al. 2007; Castillo 2012; Luscher and Malenka 2012), and signals are not restricted to the site of activation (homosynaptic vs heterosynaptic) (Hulme et al. 2014). Diffuse forms of synaptic plasticity are less well understood than site specific changes, but are important to consider when taking network physiology into consid-

eration. Changes to synaptic efficacy require significant fluctuations in Ca^{2+} signaling, generally brought about by ion flux through surface expressed receptors or by release from intracellular stores (Mulkey and Malenka 1992; Cummings et al. 1996). Short term plasticity can last from seconds to minutes, and is regularly described as post-tetanic potentiation or depression, facilitation, or augmentation. Long-term potentiation (LTP) and LTD of synaptic efficacy are changes that are generally defined to persist for hours to days post tetanus. *In vitro* slice preparations often reported long-term changes the magnitude of change relative to baseline observed at 30 or 60 minutes post-tetanus. LTD and LTP have been well described to involve cascades of signaling mechanism that are regulated by enzymatic binding kinetics and rate of change in Ca^{2+} levels, eventually signaling post-synaptic internalization of AMPARs or pre-synaptic changes to vesicle release probability. This thesis focuses on LTD, which is described as a long lasting reduction in synaptic efficacy originally proposed as a mechanism to counteract persistent potentiation of synapses (Dunwiddie and Lynch 1978). The induction of LTD is associated with slow increases to intracellular Ca^{2+} levels in the synaptic terminals that can be accomplished by evoked NT release over prolonged periods or by Ca^{2+} release from internal stores. LFS administered in the range of 1-5Hz over a period of 5 to 15 minutes is one of the most common methods for *in vitro* induction of LTD, and can induce a long lasting decrease to synaptic efficacy that is saturatable and reversible (Dudek and Bear 1992; Staubli and Ji 1996; Collingridge et al. 2010).

NMDAR dependent LTD (NMDAR-LTD) and metabotropic glutamate receptor dependent LTD (mGluR-LTD) are the two best characterized forms of LTD in the

CNS (Pöschel and Stanton 2007; Collingridge et al. 2010; Lisman 2017), each with distinct signaling pathways dependent on intracellular increases to Ca^{2+} concentrations (Mulkey and Malenka 1992; Cummings et al. 1996). Other forms of LTD are now known to develop in the presynaptic terminal by signaling through the endocannabinoid system and the cannabinoid receptor 1 (CB_1) (Castillo 2012). This type of LTD has received relatively less attention compared to the NMDAR and mGluR dependent forms of LTD, but recent advancements have indicated that this type of LTD is a much more important factor than previously thought (Navarrete and Araque 2010; Castillo et al. 2012; Suvarna, Maity, and Shivamurthy 2016; Lovinger and Abrahao 2018), especially with regards to heterosynaptic plasticity.

NMDAR-LTD is best studied in the hippocampus, between the SC of CA3 pyramidal cells and the apical dendrites of CA1 pyramidal cells (Dudek and Bear 1992; Luscher and Malenka 2012). LTD in an *in vitro* preparation was first reported in the CA1 as a decrease in synaptic efficacy induced by LFS (900x1Hz) of the SC pathway, that was sensitive to NMDA receptor inhibition by AP5, lasted for greater than one hour, and was still supportive of LTP (Dudek and Bear 1992; Mulkey and Malenka 1992). The NMDAR is often described as a coincidence detector for depolarization of the post-synaptic membrane. LFS is proposed to sufficiently depolarize the membrane to release the Mg^{2+} block in such a way that Ca^{2+} flux through the NMDAR increases intracellular Ca^{2+} levels to a degree that favours internalization of AMPARs and a decrease in the response to the stimulus. This processes is initiated at the post-synaptic density, and begins with short-term changes affecting receptor activation and sensitivity, followed by long-term changes dependent on transcription

factors, gene expression, and protein synthesis (Pöschel and Stanton 2007; Higley and Sabatini 2012 ; Luscher and Malenka 2012).

mGluR-LTD has been particularly well studied because agonist activation of mGluRs can induce a type of Chem-LTD, without having to rely on synaptic stimulation and evoked neurotransmitter (NT) release. The mGluR is a G-protein coupled receptor, and activation of the mGluR is proposed to initiate signal transduction mechanisms that promote release of Ca^{2+} from intracellular stores (reviewed in: Pöschel and Stanton 2007). In this model, post-synaptic signals are amplified by adenylyl cyclase (AC) and phospholipase C (PLC), and carried throughout the post-synaptic terminal, eventually signaling Ca^{2+} release from intracellular stores.

Various reports have indicated simultaneous mechanisms contributing to LTD at the synapse (Debanne and Thompson 1996; Oliet, Malenka, and Nicoll 1997; Muñoz et al. 2018) that are tied together by intracellular Ca^{2+} signaling and the internalization of AMPA receptors. LTD is proposed to be dependent on the activation of phosphatases, and in particular the Ca^{2+} binding phosphatase calmodulin (Coultrap et al. 2014; Luscher and Malenka 2012). The molecular mechanisms distinguishing LTD from LTP in this case are generally defined by the Ca^{2+} binding kinetics of the signaling cascades that become activated. Sufficient evidence for the involvement PKA and PKC in the expression of LTD has been shown, but the complexity of these pathways paired with multiple induction methods at individual synapses makes distinguishing origin and expression of LTD difficult.

LTP is much more dependent on the short-lived but fast increases to Ca^{2+} levels induced by high intensity and high frequency evoked stimulation protocols

(Pöschel and Stanton 2007; Luscher and Malenka 2012), and has received much more attention in the field relative to LTD. The N-methyl d-aspartate receptor (NMDAr) is tightly associated with the induction of LTP, and is commonly identified as the origin of the Ca^{2+} flux necessary for LTP (Wang, Song, and Berger 2002). This thesis focuses on the induction and expression of LTD. LTP and LTD contribute important components to the principles of learning and memory, and to date serve as some of the best neurocorrelates for studying learning and memory in a laboratory setting. All together these changes are expressed at the synapse and within individual cells to adapt and modulate response to input, in order to generate meaningful adaptations to the environment at the network level. Often summarized with Carla Shatz phrase “neurons that wire together, fire together” (Shatz 1992), the principles of synaptic plasticity are crucially important in describing and understanding the links between learning, memory, and behaviour.

The N-methyl D-aspartate Receptor

NMDA receptors are ionotropic glutamate receptors that form cation channels permeable to Na^+ , K^+ and Ca^{2+} . NMDAr receptors exist as heterotetrameric assemblies made up of two obligatory GluNR1 subunits and two more subunits from a collection of GluNR2(A-D) or GluNR3(A-B). The potential for a wide variety of diheteromeric and triheteromeric subunit combinations, along with alternative splicing and a host of post-translational modifications, cause NMDArs to exhibit a variety of gating and pharmacological properties (Erreger et al. 2005; Paoletti, Bellone, and Zhou 2013; Hansen et al. 2014). NMDArs require glutamate and a co-agonist for ac-

tivation, as well as sufficient membrane depolarization to release the Mg^{2+} channel pore block. NMDA receptors have relatively slow activation and deactivation kinetics compared to other excitatory Glu receptors such as the AMPA and kainate receptors.

NMDARs high permeability to Ca^{2+} makes them a critical component to many of the signaling mechanisms involved with synaptic plasticity. One of the NMDAR most defining properties is the Mg^{2+} block that releases with sufficient membrane depolarization. This allows ion flux only when the post-synaptic membrane is sufficiently depolarized, and is important because the Ca^{2+} permeability acts as a second messenger that initiates changes in the local synaptic density. Sufficient membrane depolarization, whether it be local synaptic depolarization or global cellular depolarization, along with calcium flux through the NMDAR, allows for a system whereby synapses can detect coincidence input and adjust synaptic strength accordingly.

Subunit variation leading to distinct combinations of diheteromeric and triheteromeric NMDAR adhere mechanistically different properties to each potential subunit combination (Erreger et al. 2005; Hansen et al. 2014; Hobbiss, Cortes, and Israely 2018). Experiments examining the decay kinetics of recombinant NMDA receptors indicate that GluN2A containing diheteromers display the fastest decay times, which are not significantly influenced by the GluN1 splice variant (Vicini et al. 1998). It is generally reported that receptors not solely comprised of GluN1/GluN2A subunits, including triheteromeric NMDARs, tend to display slower decay kinetics (Hansen et al. 2014). Other properties that could be influenced by subunit composition include desensitization, glutamate and co-agonist binding properties, Ca^{2+}

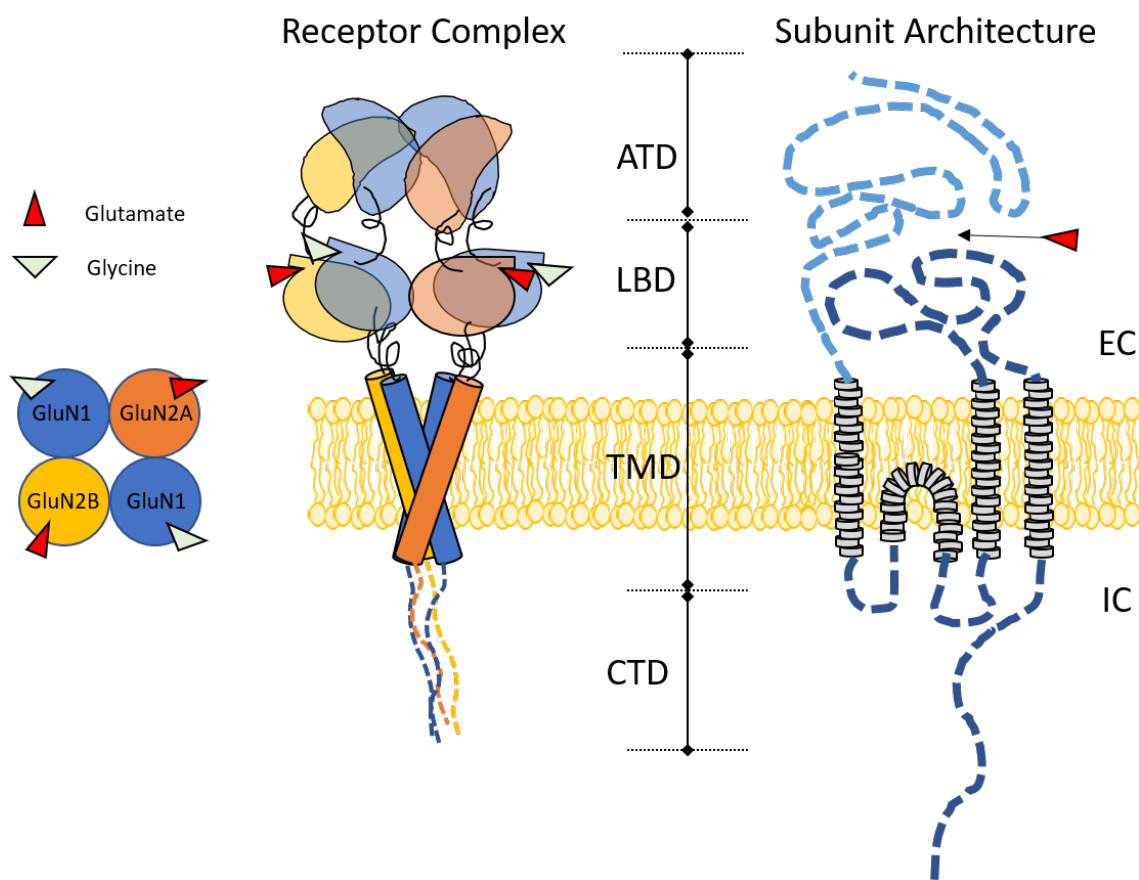


Figure 1.2: The NMDAR consists of four subunits, and is made up of two obligatory GluN1 subunits paired with two subunits drawn from a collection of GluNR2(A-D) or GluNR3(A-B). NMDAR form di or tri heteromeric complexes, each with distinct properties and gating kinetics. The GluN1 subunit binds the glycine (or d-serine) cofactor and channel opening occurs when glutamate is present and sufficient membrane depolarization release the Mg^{2+} ion blocking the pore. The NMDAR consists of the amino-terminal domain (ATD), the ligand-binding domain (LBD), the transmembrane domain (TMD), and the c-terminal domain (CTD). Each subunit passes completely through the membrane three times with a short intracellular membrane loop.

permeability & sensitivity to Mg^{2+} block, drug sensitivity, and synaptic localization (Reviewed in: Paoletti, Bellone, and Zhou 2013).

Subunits and splice variants of NMDAr have distinct spatiotemporal expression patterns in the hippocampus throughout development. In the DG, significant changes involving a redistribution of subunit density and splice variant occurs (Piña-Crespo and Gibb 2002; Coultrap et al. 2005). Early developmental periods are reported to be dominated by expression of NMDA receptors containing GluN2B subunits. As development progresses, there is a steady rise in the amount of GluN2A subunit expressed, while GluN2B expression remains relatively unchanged into adulthood (Monyer et al. 1994; Wenzel et al. 1997; Coultrap et al. 2005). Changes to the distribution and abundance of GluN2A and GluN2B subunits is likely to contribute to important developmental changes in the electrophysiological properties of cells in the DG, and be tightly related to the induction and expression of synaptic plasticity.

The acute effects of Ethanol on the NMDAr and LTD

Ethanol on the NMDAr

EtOH is the psychoactive molecule in what is colloquially referred to as alcohol. It is a widely used drug, and EtOH intoxication causes acute neurological impairment and psychoactive effects on the brain (Zorumski, Mennerick, and Izumi 2014). Excessive EtOH consumption is notorious for its ability to induce a blackout state, where the formation of new memories is impaired, despite other cognitive functions remaining intact (White et al. 2003).

EtOH is regularly reported to inhibit NMDAr currents (Lovinger, White, and Weight 1989; Lahnsteiner and Hermann 1995; Puglia and Valenzuela 2010; Hicklin et al. 2011; Wu et al. 2011; Xu et al. 2012; Hughes, Smothers, and Woodward 2013; Zhao et al. 2015), and results in the DG suggest effects similar to that observed in the CA1 (Ariwodola et al. 2003; Morrisett and Swartzwelder 1993). The acute effects of EtOH on excitatory synaptic transmission was first shown to inhibit NMDA activated currents in cultured mouse hippocampal neurons (Lovinger, White, and Weight 1989), and in the same year, EtOH was shown to both potentiate and block NMDAr single channel ion currents in cultured rat hippocampal pyramidal cells (Lima-Landman and Albuquerque 1989). EtOH is a partial antagonist of NMDAr excitatory post-synaptic currents (NMDAr-EPSCs) at a range of physiological concentrations ([1:100 mM] EtOH; BAC of 50mM ~ 0.2%) (Wright, Peoples, and Weight 1996; Ariwodola et al. 2003; Mamei 2005), and inhibition of NMDAr-EPSCs generally remains incomplete at concentrations outside the physiological range ([100:500 mM] EtOH) (Wright, Peoples, and Weight 1996; Xu et al. 2012). The effects of EtOH on NMDAr are reported to differ between potential subunit combinations (Zhao et al. 2015; Nagy 2004), and how the acute effects of EtOH on NMDAr translates into changes in the induction and expression of synaptic plasticity is still not well understood.

Ethanol and LTD

A substantial body of evidence supports EtOH inhibition of NMDAr-EPSCs (Hicklin et al. 2011; Wu et al. 2011; Xu et al. 2012; Hughes, Smothers, and Wood-

ward 2013; Zhao et al. 2015), but it is becoming clear that the effects of EtOH on NMDAR currents is not the only factor influencing the induction and expression of synaptic plasticity (Galindo, Zamudio, and Valenzuela 2005; Wu et al. 2011; Wills, Kash, and Winder 2013). The acute effects of EtOH exposure on changes to excitatory neurotransmission is best studied in the CA1, and there is overwhelmingly more research that focuses on LTP over LTD (Reviewed in: Chandrasekar 2013). EtOH regularly reduces the magnitude of LTP induced (Morrisett and Swartzwelder 1993; Izumi et al. 2005; Tokuda, Zorumski, and Izumi 2007), yet results are inconsistent with regards to concentration and magnitude of effect (Tokuda, Zorumski, and Izumi 2007). EtOH has been reported to both enhance (Hendricson et al. 2002) and inhibit (Izumi et al. 2005) the magnitude of LTD induced in the CA1 by LFS, but this has not yet been followed up on.

The Dentate Gyrus

Anatomy & Development

The DG is an evolutionarily conserved brain structure located within the hippocampus formation. The DG is made up of 3 layers (Figure 1.3); the molecular layer (ML), the granule cell layer (GCL), and the hilus. The GCL runs the entire septotemporal axis and forms the suprapyramidal and infrapyramidal blades. The blades extend along the transverse axis, separated by the hilar region, and are joined at the crest. The hilus sits abut to the CA3 pyramidal layer and contains a diverse array of excitatory and inhibitory neurons, many of which are targets for the axonal

projections leaving the GCL (Seress and Pokorny 1981).

The ML of the DG is split into the inner, middle and outer thirds. The principle source of extra-hippocampal excitatory input to the DG is the perforant path. The perforant path is subdivided into the medial and lateral axonal tracts based upon the origin of the EC axons and the termination points in the molecular layer (Witter 2007). Axons arising from the medial and lateral EC terminate on dendrites in the middle and outer third of the ML respectively. Fiber pathways projecting to the DG arises principally from layer II of the EC and traverses the pyramidal layer of the subiculum before crossing the hippocampal fissure and entering the DG. It is important to note that these layer II projections from the EC are not restricted to the DG region of the hippocampus, but also extend to the most distal region of the apical CA3 dendritic field (Amaral, Scharfman, and Lavenex 2007). DGCs display complex, dendritic trees extending from the apical portion of the cell into the molecular layer of the DG and an axon that extends out of the basal portion of the cell.

DGC axons are called mossy fibers (MF), and bifurcate extensively into multiple collaterals within the hilus before projecting to the region immediately proximal to the apical portion of the CA3 stratum pyramidale (Lynch et al. 1973). MF terminals in the hilus target a number of interneurons including excitatory mossy cells and inhibitory basket cells. The functionally and morphologically unique MF terminals were first noted by Cajal for their size, and how they made their target cells look to be covered in moss. The giant boutons are called thorny excrescences, and are unique in their morphology and plasticity (Blaabjerg and Zimmer 2007; Jaffe and Gutiérrez 2007). Thorny excrescences are much larger than most axon terminals

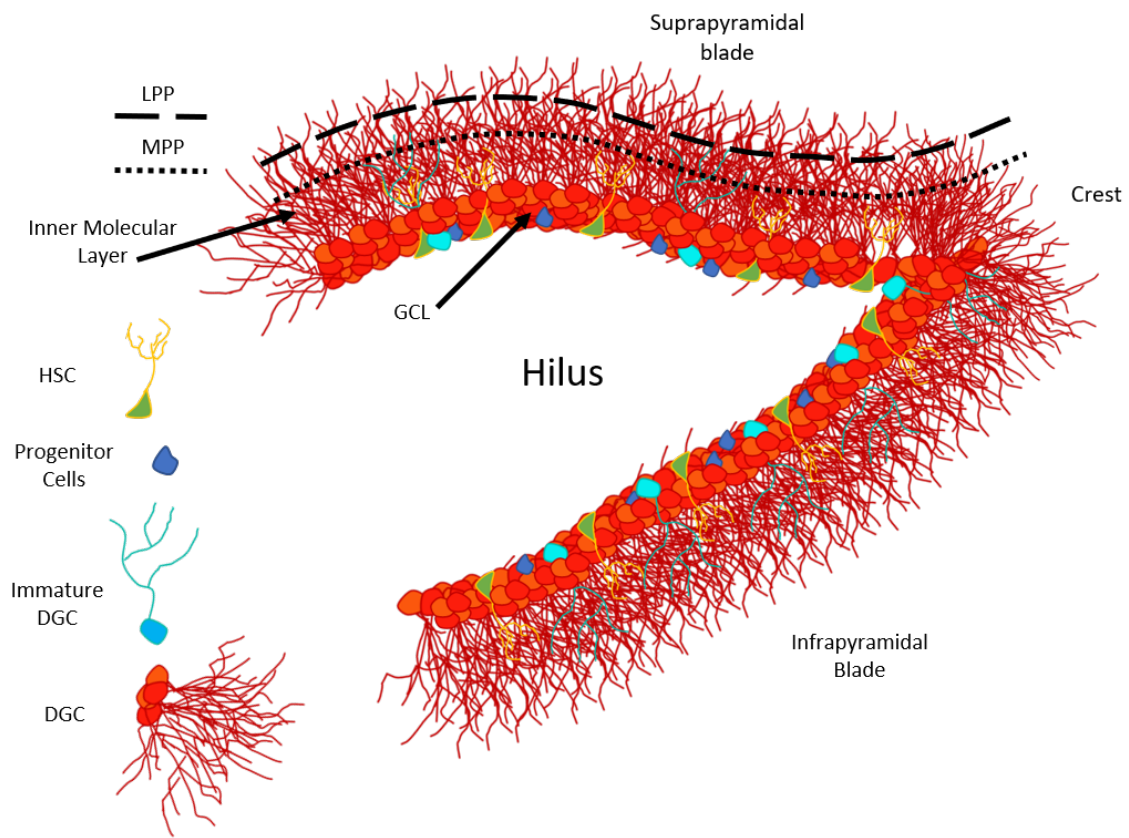


Figure 1.3: The MPP and LPP project to the middle and outer third of the molecular layer respectively. The GCL is comprised entirely of differentiated DGCs, except for at the border between the hilus and the GCL, in the subgranular zone, where new neurons are being constantly generated from a pool of progenitor cells. HSCs differentiate into progenitor cells that eventually develop into DGCs. The DG is one of only two regions of the brain identified to show persistent neurogenesis into adulthood. **Abbreviations:** Hippocampal stem cell (HSC); Dentate granule cell (DGC); Lateral perforant path (LPP); Medial perforant path (MPP); Granule cell layer (GCL)

and feature dense pools of excitatory neurotransmitter ready for release (Lawrence, Grinspan, and McBain 2004). They also undergo robust presynaptic plasticity, and have been reported to co-release GABA (Münster-Wandowski, Gómez-Lira, and Gutiérrez 2013). MFs also feature a high density of filapodial like extensions along the length of the axon that target GABAergic interneurons (Acsády et al. 1998) that provide clues as to the function of DG output to the CA3.

DG development in the rodent hippocampus begins during late embryogenesis and 80% of DGCs are formed postnatally (Liu et al. 2000). It is the last structure in the hippocampal formation to form but maintains its capacity for neurogenesis into adulthood. Formation of the GCL begins at the septal region along the septotemporal axis, forming first at the distal peak of the suprapyramidal blade and extending along the transverse axis, eventually forming the crest and turning back along the transverse axis to form the infrapyramidal blade (Rahimi and Claiborne 2007). Therefore, the most mature neurons reside in the topmost region of the SG at the most distal peak of the suprapyramidal blade, near the septal pole of the DG. The primary period of DGC neurogenesis begins in late embryogenesis and persists at a high rate until the end of the second post-natal week. Neurogenesis in the DG continues through adulthood, forming new neurons that undergo morphological development and synaptic maturation similar to that which is seen in DGCs born during the primary period of neurogenesis. The molecular layer increases in width during development from approximately $100\hat{\text{A}}\mu\text{m}$ at PND 4 to $200\hat{\text{A}}\mu\text{m}$ at PND 14, and up to $300\hat{\text{A}}\mu\text{m}$ in young adult rats.

Dentate Granule Cells

The principle cell of the DG, the dentate granule cell (DGC), differs greatly from the pyramidal cells observed throughout the rest of the hippocampus (Carnevale et al. 1997). DGCs are small (10-15 μm), ovoid cells restricted to the granule cell layer (GCL), with dendritic arbours that extend from the apical pole of the cell body into the molecular layer (ML) of the DG (Carnevale et al. 1997).

DGCs are sparse firing cells that are generated in the subgranular zone into adulthood, making the DG one of only two confirmed regions in the adult brain that undergoes neurogenesis (Gonçalves, Schafer, and Gage 2016). DGCs can be observed as early as embryonic day 14 in the rodent, and mature characteristics can be observed in the oldest DGCs as early as 1 week after birth (Pedroni et al. 2014). The most significant periods of GC development occur during the first 60 days after cell differentiation, as newborn DGCs extend dendritic arbours into the molecular layer and undergo extensive synaptic maturation and remodelling. DGCs are described as morphologically mature \sim 14 days after differentiation, once most of their dendritic arbors have extended the full width of the molecular layer. Synaptic maturation continues up to \sim 60 days after differentiation in DGCs, as they undergo significant changes to synapse density and dendritic branching before the cell is considered fully mature (Rihn and Claiborne 1990; Rahimi and Claiborne 2007).

The early developmental phase of the DGCs is generally characterized by a single, short and stubby primary apical dendrite. Immature features include numerous bifurcations characterized by growth cones, varicosities and filopodia. The most im-

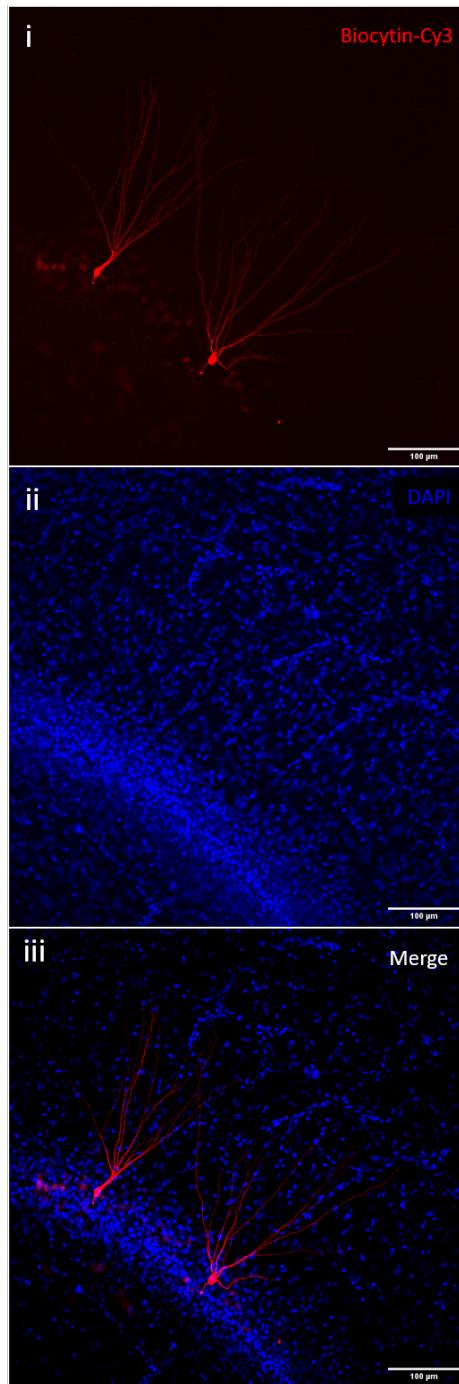


Figure 1.4: i) Two DGCs filled with biocytin projecting dendrites into the molecular layer. DGCs can be characterized by their morphological features, including the number of projections leaving the cell body, magnitude of dendritic bifurcation, and position of the cell body within the GCL. ii) DAPI stain for cell nuclei show the high density of cell bodies that make up the GCL, distinguishable as the blue segment spanning the bottom left corner. iii) Merged image showing the position of the cell bodies relative to the GCL. Image courtesy of Jenny Berrio. Scale bar represents $100\mu\text{M}$

mature DGCs may also exhibit rudimentary basal dendrites that are typically not seen on mature or healthy DGCs. The mossy fiber axon sprouts from amidst the basilar dendrites, but these features are hallmarks of immature neurons and are eventually lost as the cell matures. Extensive branching of the dendritic tree and formation of distinct spines in place of filopodial like extensions occurs during the initial maturation phase. After the first week, DGCs begin to show the hallmark bifurcation of the primary dendrites as the neuron's arbors extend towards the outer edge of the ML and form their characteristic dendritic tree. By 14 days after birth, DGCs express few of the growth cones, varicosities and filopodia like extensions described in the most immature DGCs, and their dendritic arbors generally reach all the way to the edge of the molecular layer. By this time, DGCs have dendritic trees for which the total length is not significantly different compared to the total dendritic length of mature DGCs, though the number of dendritic segments has been shown to be decreased in mature DGCs (aged 50- to 60- days old) when compared to young DGCs (14- to 19- days old). After the first two weeks of morphological development, the cell continues to mature, undergoing extensive synaptic modifications until the neuron reaches ~60 days of age. The final stages of DGC development are characterized by robust changes to dendritic features and synaptic density as the newly born neuron integrates into the local network. (Fricke and Prince 1984; Ye et al. 2000; Liu et al. 2000). DGCs are born at the border separating the DGL and the hilus at the subgranular zone (SGZ), and, throughout maturation the cell soma follows the path of its apical dendrites from the SGZ towards the molecular layer. It appears that adult born DGCs undergo similar developmental phases as those born in late embryogene-

sis or during the peak neurodevelopmental period (Beining et al. 2017).

Mature DGCs exhibit extensive dendritic branching observed to the magnitude of the 7th order. Their total dendritic length can extend over $3000\mu\text{M}$ into the molecular layer and bridge $\sim 300\mu\text{M}$ along the transverse axis (Felthouser and Claiborne 1990; Rahimi and Claiborne 2007). It is interesting to note that neurons of the suprapyramidal blade exhibit, on average, greater overall total dendritic length, and a greater width along the transverse axis. These morphological characteristics decline on average when moving along the transverse axis towards the crest and then back along the infrapyramidal blade.

Long-Term Depression in the DG

Relatively little work has gone into DG-LTD as compared to other regions of the hippocampus, and this is reflected in the current understanding of the mechanisms involved in the induction and expression of DG-LTD (For review see: Pöschel and Stanton 2007). LTD can be induced a variety of ways at DG-MPP synapses, and the mechanisms involved are still not fully understood. Reports on the induction and expression of *in vitro* DG-LTD have described significant roles for mGluRs (Trommer, Liu, and Pasternak 1996, Camodeca et al. (1999)), NMDARs (Christie and Abraham 1992b; Desmond et al. 1991; O'Boyle et al. 2004; Wu et al. 2001), voltage gated Ca^{2+} channels (Christie and Abraham 1992b), and the EC system (Chávez, Chiu, and Castillo 2010; Castillo et al. 2012). Clues as to the morphological role of synaptic depression in the DG come from *in vivo* work that has shown activity dependent pruning of synapses in response to input associated with decrease

in synaptic efficacy (Mezey et al. 2004; Medvedev et al. 2010; Henson et al. 2016). DG-LTD is generally induced by LFS or by acute application of various neuromodulators (LTD_{Chem}). DG-LTD is likely expressed through a variety of different induction mechanisms activated simultaneously (Pöschel and Stanton 2007; Lisman 2017).

LTD_{Chem} is readily inducible by acute application of group 1 mGluR agonists such as DHPG, and is expressed by the internalization of AMPA receptors through mechanism dependent on the release of Ca^{2+} on internal stores. Occlusion experiments have provided strong evidence that mGluR-LTD is also readily induced with LFS (Wang, Rowan, and Anwyl 1997), with significant reductions in synaptic efficacy measuring 20-40% of baseline. Many reports have suggested that this effect occurs independently of NMDAR activation (S M O'Mara, Rowan, and Anwyl 1995; Trommer, Liu, and Pasternak 1996; Wang, Rowan, and Anwyl 1997; Camodeca et al. 1999). While there is sufficient evidence to support NMDARs playing a role in the induction and expression of DG-LTD (O'Boyle et al. 2004; Desmond et al. 1991; Wu et al. 2001), to what extent they are involved remains relatively unclear. NMDARs provide quick significant changes in the intracellular concentrations of Ca^{2+} , and have a well documented role in DG-LTP and in other forms synaptic plasticity characterized throughout the brain (Pöschel and Stanton 2007).

The EC system has generated a lot of attention lately for its role in DG-LTD. EC-LTD has been closely linked to another recently described form of LTD_{Chem} in the DG that is dependent on activation of transient receptor potential (TRPV1) with capsaicin. This novel LTD_{Chem} is modulated by the endogenous cannabinoid

anadamide, and has been described to involve a Ca^{2+} -calcineurin dependent cascade leading to the post-synaptic internalization of AMPA receptors (Chávez, Chiu, and Castillo 2010). These methods of induction share many of the same principles of induction as other forms of LTD, including proposed increases to intracellular Ca^{2+} in the pre-synaptic and post-synaptic terminals to promote changes to pre-synaptic vesicle release and a desensitization to the glutamate response. This ultimately leads to long term structural changes at the post-synaptic density (Medvedev et al. 2010), and changes to synaptic efficacy led by the internalization of AMPA receptors (Wilkerson, Albanesi, and Huber 2018; Chávez, Chiu, and Castillo 2010).

Neurophysiology in the DG

Neurophysiology aims to characterize ionic conductance across the membrane, through the many unique receptors expressed in neurons. The study of synaptic plasticity examines how membrane conductance can be modulated by changes to receptor sensitization and/or density in the pre and post synaptic terminals. The fundamentals of neuronal communication are governed by Ohms law ($V = IR$), and significant advancements in the study of neurophysiology and synaptic plasticity have been made since Hodgkin and Huxley were first able to measure ionic flux across the membrane of the squid giant axon (Hodgkin and Huxley 1945). Glutamatergic excitatory neurotransmission makes up the bulk of excitatory signaling in the central nervous system (CNS). Activation of glutamate receptors can stimulate neuronal membrane depolarization by enabling cation flux through the α -amino-3-hydroxy-5-methyl-4-isoxazolepropionic acid receptor (AMPAr). Inhibitory neurotransmission on the other

hand relies on Cl^- flux through the γ -aminobutyric acid receptor (GABA_A), and generally opposes eNT by hyperpolarizing the cell membrane. Modulation of excitatory and inhibitory neurotransmission makes up the groundwork for the experimental analysis of changes to synaptic efficacy. *In vitro* electrophysiology is often employed as a means for investigating the molecular mechanisms of synaptic plasticity because of the ability to tightly control experimental conditions. Induced changes to synaptic efficacy at excitatory synapses are routinely characterized by changes to the excitatory post-synaptic potentials (EPSP) (Figure 1.5A) and the excitatory post-synaptic currents (EPSC) (Figure 1.5D) generated by neurons as electrical signals are converted to chemical signals then back again to electrical (Kandel and Spencer 1968). Changes to synaptic efficacy can be experimentally induced by stimulating bundles of axons to evoke neurotransmitter release at the synapse, or by transient receptor activation using neuromodulators. This thesis utilizes *in vitro* field and patch clamp electrophysiology to study the acute effects of EtOH on DG-LTD_{LFS} (900x1Hz), and NMDAr-EPSCs.

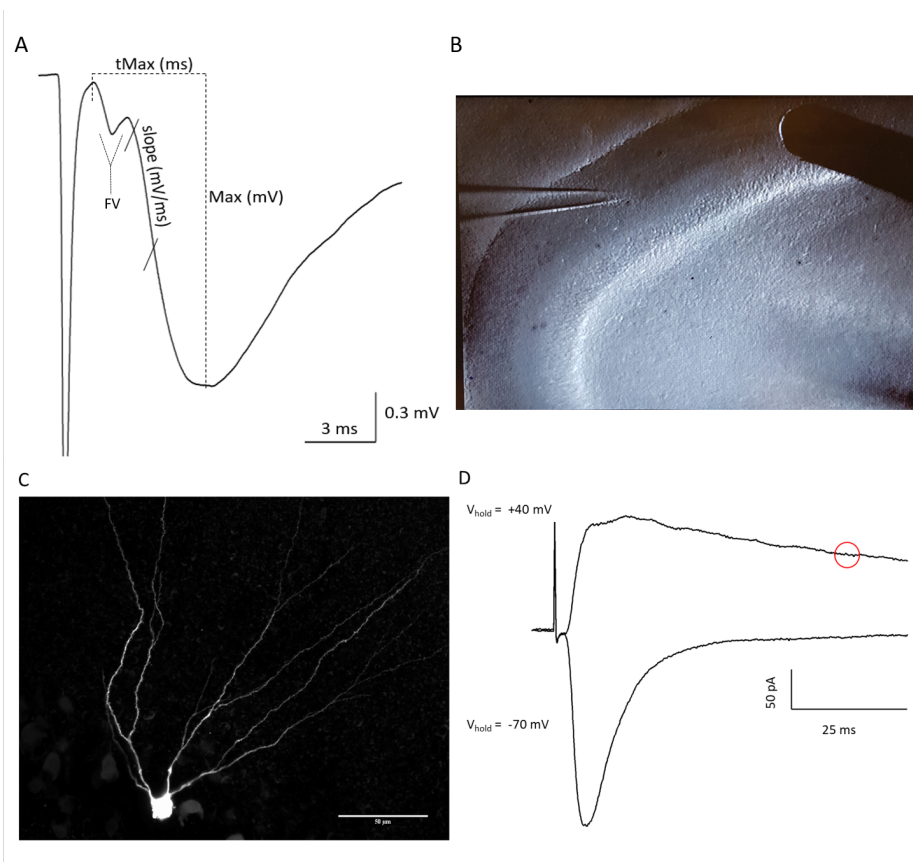


Figure 1.5: Two common methods of analyzing neurophysiology. A) An example trace of an evoke EPSP. EPSPs are principally analyzed for the immediate rising phase of the observable voltage deflection following the fiber volley (FV). The initial EPSP slope is considered to be representative of opening of AMPAR channels in response to NT. Changes in this region are proposed to reflect changes in the sensitivity or density of AMPA receptors in the post-synaptic region. The FV is representative of the change in voltage that occurs as axons release neurotransmitter from the pre-synaptic terminal. B) Placement of the stimulating electrode (left) and the recording electrode (Right) into the middle of the ML to stimulate the MPP, and record the subsequent EPSP generated in the dendritic field of an entire population of DGCs. C) Whole-cell patch-clamp electrophysiology can be used to isolate individual neurons amidst a population, to collect data on how individual neurons respond to stimuli. High resistance seals created between a small diameter (1-4 μM) glass pipette tip and the cell membrane, make it possible to create a continuous circuit by breaking the cell membrane under the pipette tip while maintaining the high resistance seal at the edges. This neuron was filled with biocytin during the experimental procedure, and later conjugated to the fluorescent marker Cy3 for imaging. D) Example traces of EPSCs collected in voltage-clamp mode from a single DGC in whole-cell patch-clamp configuration. Rapid transitions between measuring the cell's membrane voltage and injecting current make it possible to hold a cell at a pre-determined voltage and measure the current flux through receptors in response to evoked NT release. At resting membrane potential (-70mV), the EPSC is primarily representative of ionic flux through AMPARs. NMDAR-EPSCs can be isolated from AMPAR-EPSCs by holding the cell at a positive membrane potential (+40mV) to release the Mg^{2+} block, and taking advantage of the slow receptor kinetics compared to AMPARs. In this experiment, NMDAR-EPSCs were measured by analyzing the current flux 50ms after the onset of the EPSC. At this point, AMPA receptors are closed and no longer passing current across the membrane. DGC image courtesy of Armin Bayati

CHAPTER 2

Materials and Methods

Subjects:

Sprague Dawley rats from both sexes were either bred in house or obtained through Charles Rivers (Ontario, Canada). The day of birth was considered PND0 and pups were weaned at post natal day (PND) 21. Age groups selected for were made up of rats aged 13-15, 20-22, and 27-30, and are subsequently referred to as PND14, PND21, and PND28 respectively. Rats were housed in polyethylene cages with red polyethylene housings and given *ad libitum* access to standard rat chow. Subjects were kept on a 12-hour light/dark cycle in a room with a constant ambient temperature of 21 ± 1 °C and humidity $50\% \pm 7\%$. The average weights of rats (in grams) were 31.83 ± 0.67 , 56.69 ± 1.08 , and 98.61 ± 1.49 for each age group respectively. ANOVA revealed no significant differences in the weight of subjects within groups.

Tissue Preparation:

All solutions were bubbled continuously throughout the day with carbogen ($95\%O_2 / 5\%CO_2$). Slices for field electrophysiology were cut, incubated and perfused in either oxygenated artificial cerebral spinal fluid (aCSF) containing (in mM): 125 NaCl, 2.5 KCl, 1.25 NaHPO₄, 25 NaH₂CO₄, 2 CaCl₂, 1.3 MgCl₂, and 10 dex-

trose (295-305 mOsm; pH of 7.3) or in a high sucrose cutting solution containing (in mM): 200 Sucrose, 2.5 KCl, 1.25 NaH₂PO₄, 25 NaHCO₄, 0.5 CaCl₂, 7 MgCl₂, 10 dextrose, 1 Ascorbic Acid, and 3 Na-pyruvate. All slices for patch-clamp electrophysiology were cut in the high sucrose solution.

Rats were anaesthetized with isoflurane and swiftly decapitated for brain excision. The brain was exposed by making a shallow cut along the mid sagittal plane past bregma and peeling the parietal bone the along the coronal suture to expose the cerebral hemisphere and olfactory bulbs. Brains were removed and immediately submerged in ice cold cutting solution for 30 seconds to a minute. Tissue was prepared for sectioning by first removing the cerebellum and the prefrontal cortex then splitting each hemisphere along the midline with a longitudinal cut. Hemispheres were rotated to their midsagittal side and a section of tissue was removed from the dorsal cerebrum at an approximate angle of $\sim 25^\circ$ relative to the base cutting surface, and $5-15^\circ$ along to the rostral-caudal axis. Each cerebral hemisphere was then transferred to dry filter paper before the cut dorsal surface was glued to a stage for sectioning. $350\mu\text{m} - 400\mu\text{m}$ transverse slices were cut in solution at approximately $2-4^\circ\text{C}$ using a vibratome (1500 Ted Pella, Inc., CA, USA) and immediately transferred to solution held at 32°C . Slices were left to incubate for 30 minutes before switching off the water bath. Slices were left for a minimum of 30 minutes before being transferred to a recording chamber.

Extracellular field electrophysiology:

fEPSPs were recorded from the suprapyramidal blade of the DG. Slices were visualized under an upright fixed stage Olympus BX51W1 microscope and perfused with oxygenated aCSF (95% O₂/5% CO₂) at 2-3 mL/min at 29.9 °C +/- 1 °C. Pipette tips (500kΩ â 2 MΩ.) were pulled with a Sutter P-1000 micropipette puller and filled with perfusion media. Stimulating electrodes (concentric bipolar pt/ir; FHC, Bowdoin, ME, USA) were placed into the middle third of the molecular layer, paralleled by the hippocampal fissure and the GCL to stimulate the MPP. fEPSPs were recorded from the dendritic field adjacent to the stimulating electrode along the transverse axis in the middle third of the molecular layer.

IO curves were generated by delivering square current pulses at a rate of 0.1Hz at sequentially increasing pulse widths (30 μ s to 300 μ s). All other protocols utilized in data acquisition employed a pulse width of 120 μ s, and fEPSP response was adjusted by changing the amplitude of the current pulse. Following IO responses, paired pulses separated by 50ms were delivered at a rate of 0.667Hz. The experimental EPSP (ExPSP) was acquired by adjusting the amplitude of the current pulse to produce a fEPSP 60-80% of the maximum. Evoked responses were acquired at a rate of 0.0667Hz and ExPSP were left to settle for a minimum of 20 minutes before any drug wash in or tetanus. LFS was induced at the same current amplitude and pulse width (900x1Hz; pulse width of 120 μ s) as baseline. Unless otherwise stated, drug application was restricted to a maximum exposure time of 5 minutes before LFS, remained in the bath for the duration of the stimulation protocol, and was washed out

after the LFS was complete. LTD (represented as percent change from baseline) was analyzed by comparing the fEPSP slope at minutes 55-60 of an hour long decay, to the slope collected during 5-minutes preceding the conditioning stimulus.

Analysis of fEPSP slope

Slope was calculated by examining the initial rising phase of the fEPSP. The initial rising phase was chosen to isolate the monosynaptic response from the fiber volley and avoid contamination of the signal by disynaptic components. The fEPSP was analyzed three different ways. Custom written data analysis software utilizing the R programming language (R Core Team 2018) provided the means for analysis of the fEPSP. The method of analysis included in the final analysis was determined by observations related to the baseline, and observable changes to the fEPSP that were seen after the decay period that had the potential to influence the slope, including changes to the intersection point between the fEPSP and the fiber volley. Briefly, each piece of data was first analyzed by calculating the x-axis values that represented 10% and 50% points of the observable voltage deflection of the EPSP as determined by the representative averaged trace from the 20 sweeps (5 minutes) before conditioning. A linear model was then fitted to the data for each individual sweep between these two fixed points. The second method of analysis utilized R to determine the rate of change for each sample in the sweep to map the first derivative of the slope to the rising phase of the EPSP. This allowed for analysis of how the maximum calculable slope of the EPSP was affected by LFS. The third method of analysis employed determined the slope of the data between 20% and 60% of the

maximum EPSP (relative to 0mV) for each individual sweep. This floating point method was employed to ensure that the slope was accurately calculated for, independent from changes to the maximum EPSP and changes to the observable voltage deflection. 20% and 60% were chosen because this method of analysis calculated the points based upon the maximum voltage deflection relative to zero, and therefore had to take the voltage deflection of the fiber volley into consideration.

Every effort was made to include each potential piece of data. Baseline stability was the major determining factor when selecting which method of analysis best represented the data, and the analysis with the lowest slope coefficient was most often chosen to represent the collected data. Slices were omitted if the fitting a linear regression model to the 15 minutes of baseline preceding conditioning stimulus resulted in a slope coefficient with an absolute value greater than 0.75 for all three possible methods of analysis. Other instances that permitted slices to be omitted revolved around issues related to bath temperature and flow.

Evoked responses were amplified with either an Axopatch 200B or Multiclamp 700B and filtered at 10kHz with a low-pass Bessel filter and digitized at a rate of 100kHz ($10\mu s$) (Digidata1440 & 1550b).

Whole-cell patch clamp electrophysiology:

Visualized whole-cell recordings were made in a modified aCSF containing (in mM): 119 NaCl, 3 KCl; 1.25 NaHPO₄; 25 NaH₂CO₄; 1.3 CaCl₂; 1 MgCl₂; 10 dextrose; 1 Ascorbic Acid; and 3 Na-pyruvate (295-305 mOsm; pH of 7.4). Pipette tips (4â “6M Ω .) were pulled with a Sutter P-1000 micropipette puller and filled with in-

tracellular pipette solution containing (in mM): 123 CsMeSO₄; 7 CsCl; 5 EGTA; 10 HEPES; 1 CaCl₂; 5 Phosphocreatine Tris; 3 MgATP, 0.2 GTP Tris, 5 QX-314 Bromide (285 mOsm, pH 7.3). Picrotoxin (100 μ M in DMSO) was added to the modified aCSF to block fast inhibitory GABAA channels. Excitatory post-synaptic conductance's (EPSCs) were recorded from DGCs located in the suprapyramidal blade of the DGL. Slices were visualized under an upright fixed stage Olympus BX51W1 microscope and perfused with modified aCSF, oxygenated with 95% O₂/5% CO₂ at 2-3 mL/min at 32°C +/- 1°C.

Cell access was obtained in voltage-clamp mode after acquiring seals > 1G Ω . DGCs were voltage-clamped at \hat{a} -70 mV \hat{a} or '+40mV' for AMPAr and NMDAr responses respectively after correcting for the liquid junction potential . EPSC responses were adjusted to 40-60% of their maximal AMPAr response by adjusting the amplitude of a 0.12 ms current pulse. Evoked responses were collected at a rate of 0.0334Hz and EPSCs were elicited by stimulation of the MPP similar to as described above. NMDAr-EPSCs were isolated by stepping the cell to +40mV before stimulation and currents were analyzed 50ms after the onset of current flux. Passive electrical properties of the cell were monitored with a 5mV hyperpolarizing test pulse. Series resistance (R_s) was not compensated for. Cells with R_s > 30M Ω , or that showed changes to the R_s > than 20% were omitted.

Evoked responses were amplified with an Axopatch 200B and filtered at 2kHz with a low-pass Bessel filter and digitized at a rate of 10kHz (100 μ s) (Digidata1440 & 1550b).

Drugs

All drugs were purchased from Sigma-Aldrich (St. Louis, MO) or Tocris Biosciences (Burlington, ON). EtOH (95%) was acquired from the university stores facility and added to solution immediately before wash in. Stock solutions of DL-AP5 (10mM) were made in distilled water and stored at -20°C.

Statistics

Statistics were computed using the R-Project for statistical computing (R Core Team 2018). Packages utilized for the analysis and presentation of data include ggplot2 (Wickham 2016), gginnards (Aphalo 2018), data.table (Dowle and Srinivasan 2019), kableExtra (Zhu 2019), knitr (Xie 2018), lme4 (Bates et al. 2019), PNG (Urbanek 2013), rMarkdown (Allaire et al. 2018), roxygen2 (Wickham, Danenberg, and Eugster 2018), tidyverse (Wickham 2017), usethis (Wickham and Bryan 2018) and yaml (Stephens et al. 2018). All data are presented as mean +/- standard error of the mean (SEM). Statistical differences were determined by two-tailed student t-test or one-way analysis of variance (ANOVA) followed by the appropriate post-hoc test. The level for statistical significance was $p < 0.05$.

CHAPTER 3

Results

No significant change in the magnitude of DG-LTD_{LFS} between PND 14, 21, and 28.

LFS (900x1Hz) at DG-MPP synapses administered at a stimulus intensity and with a pulse duration that was unchanged from baseline consistently induced a reliable decrease in the fEPSP slope at PND14 (-15.08 +/- 1.76 %, slices = 22, animals = 12), PND21 (-14.31 +/- 2.53 %, slices =24, animals = 13), and PND28 (-12.14 +/- 1.75 %, slices =35, animals = 15) (Figure 3.1). No significant differences were seen in the magnitude of LTD induced at each age group as determined by one way ANOVA ($F_{(2,78)} = 0.611$, $p = 0.55$). One way ANOVA revealed no significant differences in the magnitude of LTD induced when subjects were grouped by sex ($F_{(1,79)} = 0.008$, $p = 0.93$).

A decrease in the slope of the fEPSP greater than 10% of baseline was observed in 86.36%, 58.33%, and 60 % of slices at PNDs 14, 21 and 28 respectively, and a percentage of slices in each age group (PND14: 4.55%, PND21: 4.17%, and PND28 17.14%) showed a potentiation of the EPSP slope after LFS. No slices showed a potentiation of the EPSP slope greater than 10% in any age group.

A certain number of slices from age groups PND21 ($n = 5$) and PND28 ($n = 12$) were cut in a high sucrose cutting solution (Figure 3.1: F,G). Age groups were

pooled and control data was randomly sampled to equal the number of slices in the sucrose group. No significant differences were observed in the magnitude of LTD induced when cutting in high sucrose solution compared to cuts done in regular ACSF (Sucrose: $-13.37 \pm 2.3\%$, rACSF: $-12.61 \pm 2.33\%$; pairwise t-test, $p = 0.48$).

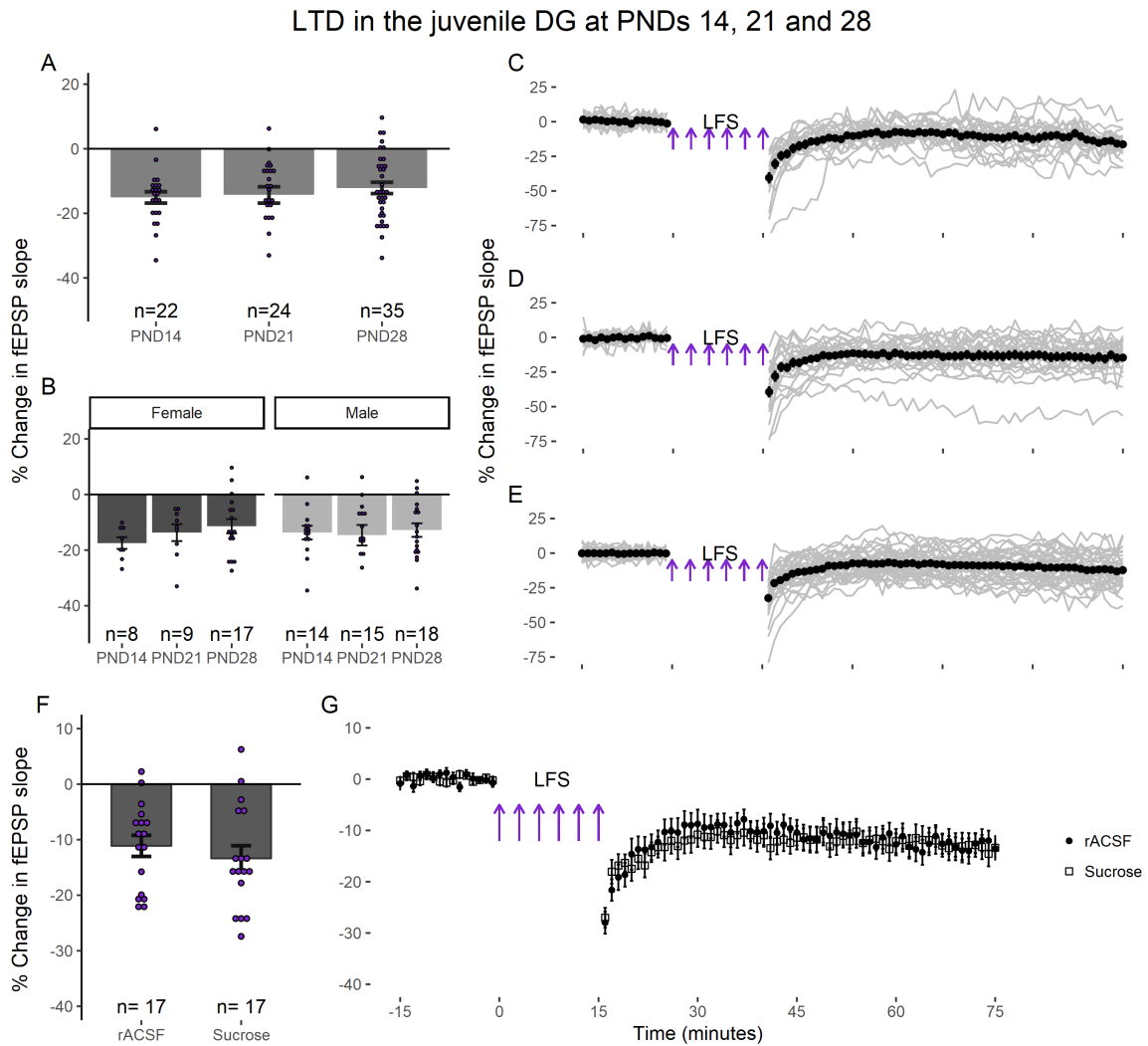


Figure 3.1: LFS (900x1Hz) regularly induced depression of the fEPSP at each point throughout the jDP. (A) LFS induced a decrease in the fEPSP that was greater than 10% in 87%, 59%, and 60% of slices at PND14, 21 and 28 respectively. This was not associated with a statistically significant difference in the magnitude of LTD induced between groups. (B) No significant effect of sex was seen when age groups. (C,D,E) Representative figures showing the induction and expression of LTD after LFS for PND14 (C), PND21 (D), and PND28 (E) age groups respectively. LTD was observed by comparing the 5 minutes preceding LFS to the last 5 minutes of a 60 minute decay. (F,G) Slices cut in a high sucrose cutting solution had no significant effect on the magnitude of LTD induced after LFS.

AP5 inhibits DG-LTD_{LFS} at PND21 and PND28, but not at PND14

To get a better understanding of how NMDARs affect LFS-LTD in the DG, and to determine if development plays a role acute sensitivity to AP5, LFS was induced in the presence of 50 μ M AP5. LFS induced in the presence of AP5 showed a change in the fEPSP slope from baseline that measured -14.03 \pm 1.9 %, at PND14 (slices = 9, animals = 7), 0.14 \pm 3.19 % at PND21 (slices =15, animals = 7), and 0.75 \pm 3.69 % at PND28 (slices =10, animals = 5) (Figure 3.2). Two way ANOVA revealed a significant interaction of age and treatment ($F_{(2,109)} = 3.37$, $p = 0.038$). Follow up post-hoc analysis revealed a significant effect of treatment with AP5 at PND21 and PND28 ($p = 0.0011$, $p = 0.0016$; post-hoc pairwise comparisons with Bonferroni correction), and significant differences in the effects of AP5 between the early juvenile time period (PND14), and the late juvenile groups (PND21: $p = 0.012$, PND28: $p = 0.017$; post-hoc pairwise comparisons with Bonferroni correction).

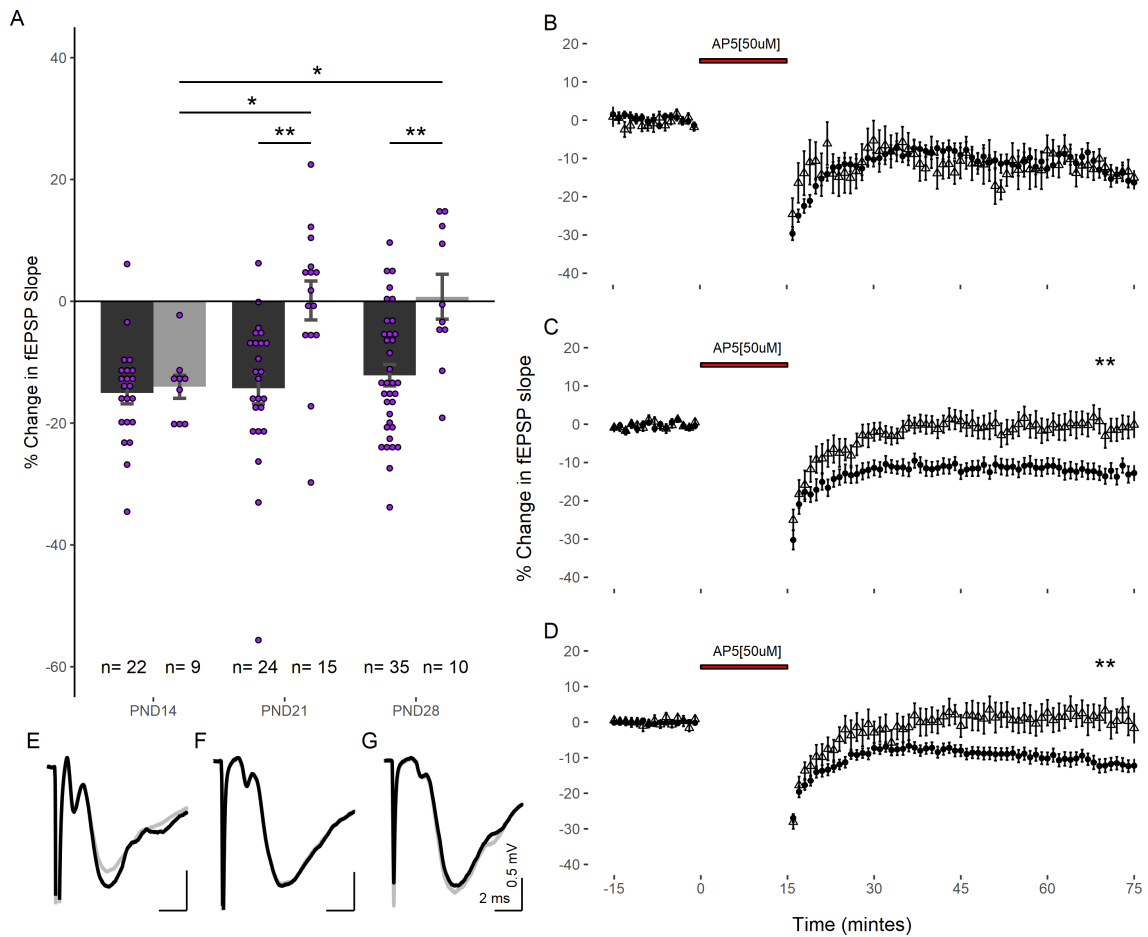


Figure 3.2: LFS (900x1Hz) in the presence of AP5 significantly inhibited LTD in the PND21 and PND28 groups, but had no effect at PND14. (A) Significant differences were observed between the effects of AP5 when comparing the early juvenile group (PND14) to the PND21 and PND28 groups ($p = 0.01$). (B,C,D) Representative figures showing the induction and expression of LTD after LFS, and the effects of AP5 on recovery of the response for PND14, PND21, and PND28 age groups respectively. Statistically significant differences were observed by comparing the 5 minutes preceding LFS to the last 5 minutes of a 60 minute decay. (E,F,G) Representative traces of the fEPSP before conditioning (black), and after a 60 minute decay period (grey) for PND14, PND21, and PND28 age groups respectively. Scale bars represent 2ms and 0.5mV for each trace.

50mM EtOH attenuates DG-LTD_{LFS} at all points in the jDP

To examine if acute EtOH application during LFS affects DG-LTD_{LFS} in a developmentally regulated fashion, LFS was induced at DG-MPP synapses in 50 and 100mM EtOH, and all three age groups were examined for the % change in the fEPSP slope 60 minutes after the end of the conditioning stimulus. The duration EtOH exposure has been proposed to affect the expression of synaptic plasticity (Tokuda, Zorumski, and Izumi 2007), so care was taken to ensure that slices were exposed to EtOH for no more than 5 minutes before the conditioning stimulus. EtOH was added to the perfusate immediately before switching solutions to minimize the potential for variation in the EtOH concentration, due to the high volatility of EtOH. LFS of DG-MPP synapses in the presence of 50mM EtOH induced LTD that measured $-7.47 \pm 3.45\%$, $-6.52 \pm 3.15\%$, and $-5.03 \pm 1.5\%$ of baseline at PND14, PND21, and PND28 respectively (Figure 3.3). Two way repeated measures ANOVA revealed a significant main effect of treatment with 50mM EtOH on the magnitude of LFS-LTD induced ($F_{(1,105)} = 11.37$, $p = 0.001$) compared to controls, and no significant effect of age ($F_{(2,105)} = 0.769$, $p = 0.466$). Follow up post-hoc analysis showed 50mM EtOH significantly inhibited DG-LTD_{LFS} at PND14 ($p = 0.048$) and PND28 ($p = 0.043$), with a trend towards inhibition at PND21 ($p = 0.069$; post-hoc pairwise comparisons with Bonferroni correction). Treatment with EtOH[50mM] at PND21 potentiated the response in ~40% of slices, while the effects of EtOH[50mM] at PND28 showed a reduction in the variability of LTD expressed.

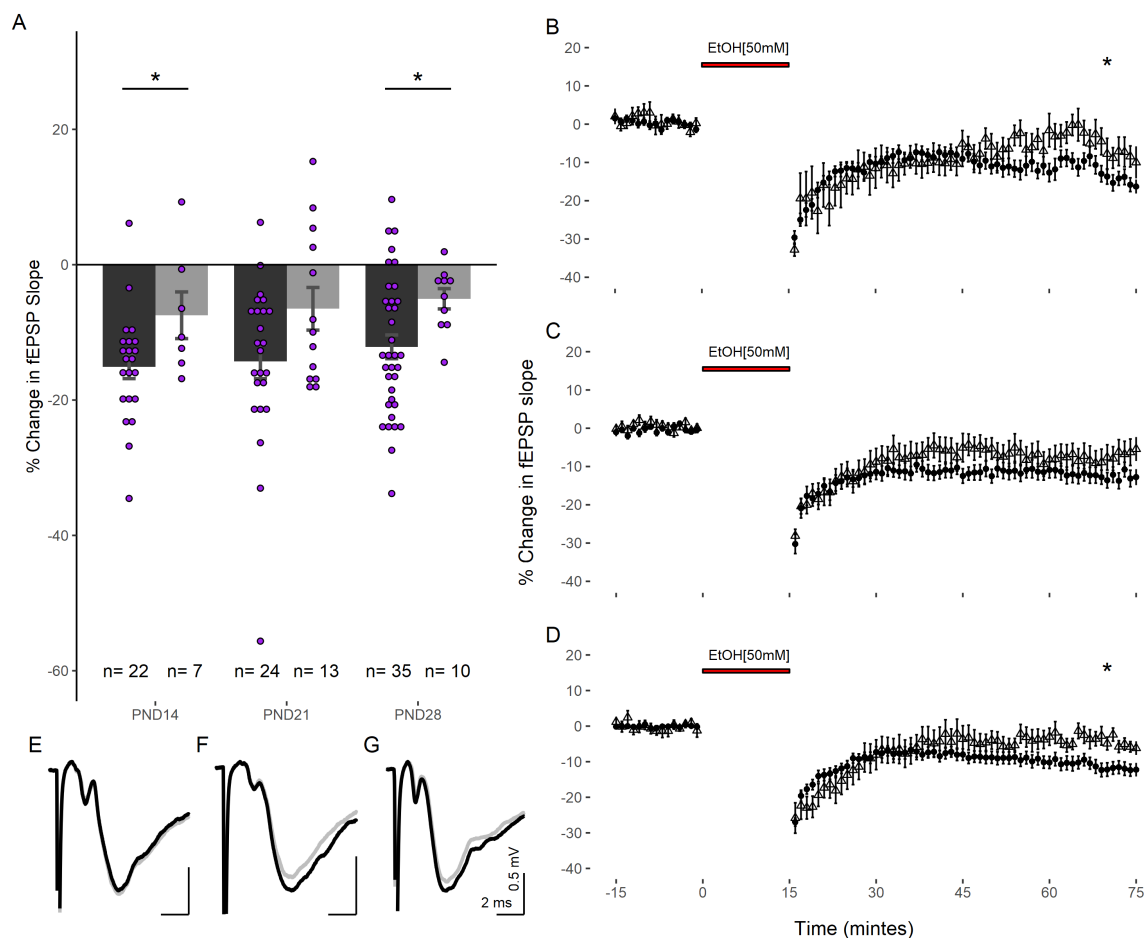


Figure 3.3: LFS (900x1Hz) in the presence of 50mM EtOH significantly inhibited LTD at PND14 and PND28, but the effects at PND21 were not significant. (A) No significant differences were observed when comparing the effects of 50mM EtOH between age groups. (B,C,D) Representative figures showing the induction and expression of LTD after LFS in the presence of 50mM EtOH for PND14, PND21, and PND28 age groups respectively. The expression of LFS was determined by comparing by comparing the 5 minutes preceding LFS to the last 5 minutes of a 60 minute decay. (E,F,G) Representative traces of the fEPSP before conditioning (black), and after a 60 minute decay period (grey) for PND14, PND21, and PND28 age groups respectively. Scale bars represent 2ms and 0.5mV for each trace.

100mM EtOH has no significant effect on DG-LTD_{LFS} at any point throughout the jDP period

LFS to DG-MPP synapses in 100mM EtOH resulted in LTD that measured -16.65 +/- 3.31%, -10.94 +/- 3.31%, and -7.55 +/- 4.03% of baseline at PND14, PND21, and PND28 respectively (Figure 3.5). Statistical analysis of the effects of 100mM EtOH on DG-LTD_{LFS} with a two-way ANOVA revealed no significant effect of treatment ($F_{(1,105)} = 1.887$, $p = 0.172$) or age ($F_{(2,105)} = 0.449$, $p = 0.639$).

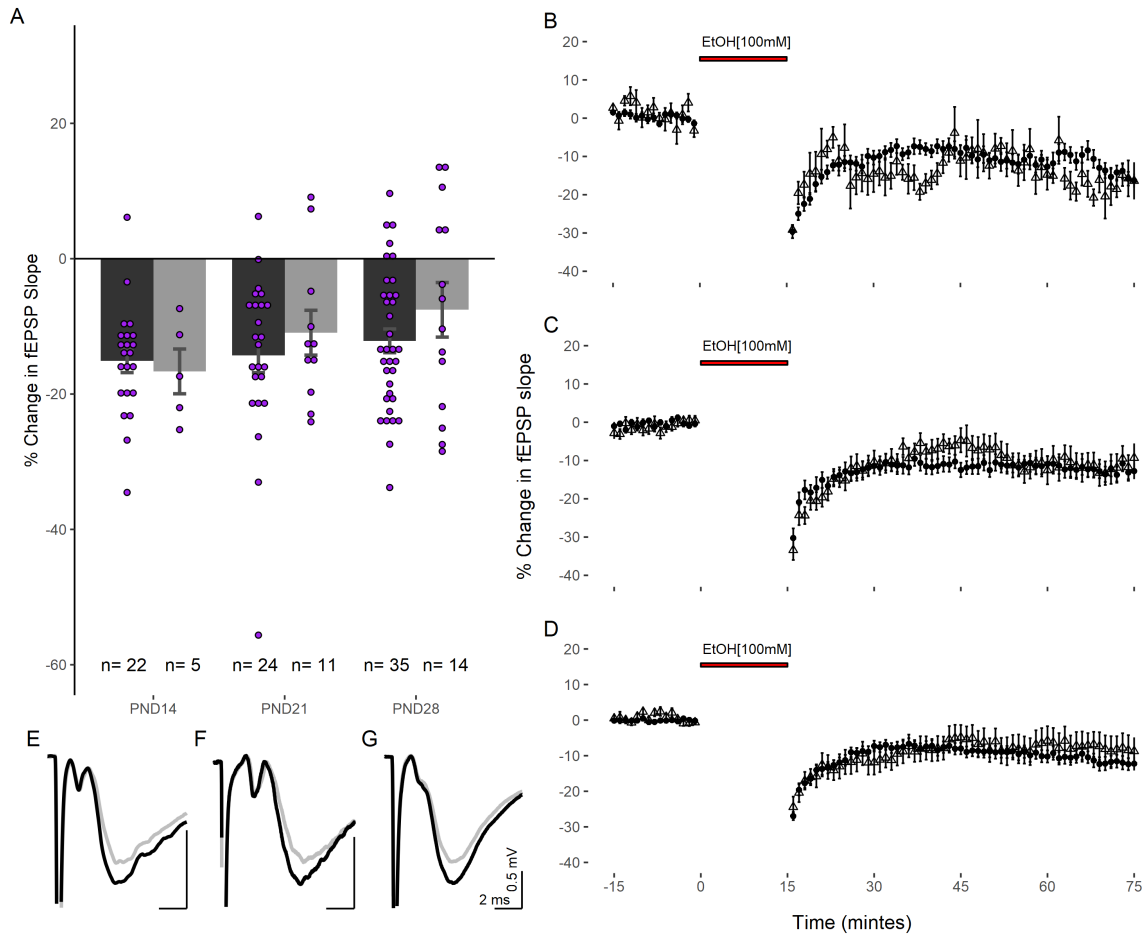


Figure 3.4: LFS (900x1Hz) in the presence of 100mM EtOH did not significantly affect LTD at any time point. (A) LFS reliably induced LTD at each time point. (B,C,D) Representative figures showing the induction and expression of LTD after LFS in the presence of 100mM EtOH for PND14, PND21, and PND28 age groups respectively. The expression of LFS was determined by comparing by comparing the 5 minutes preceding LFS to the last 5 minutes of a 60 minute decay. (E,F,G) Representative traces of the fEPSP before conditioning (black), and after a 60 minute decay period (grey) for PND14, PND21, and PND28 age groups respectively. Scale bars represent 2ms and 0.5mV for each trace.

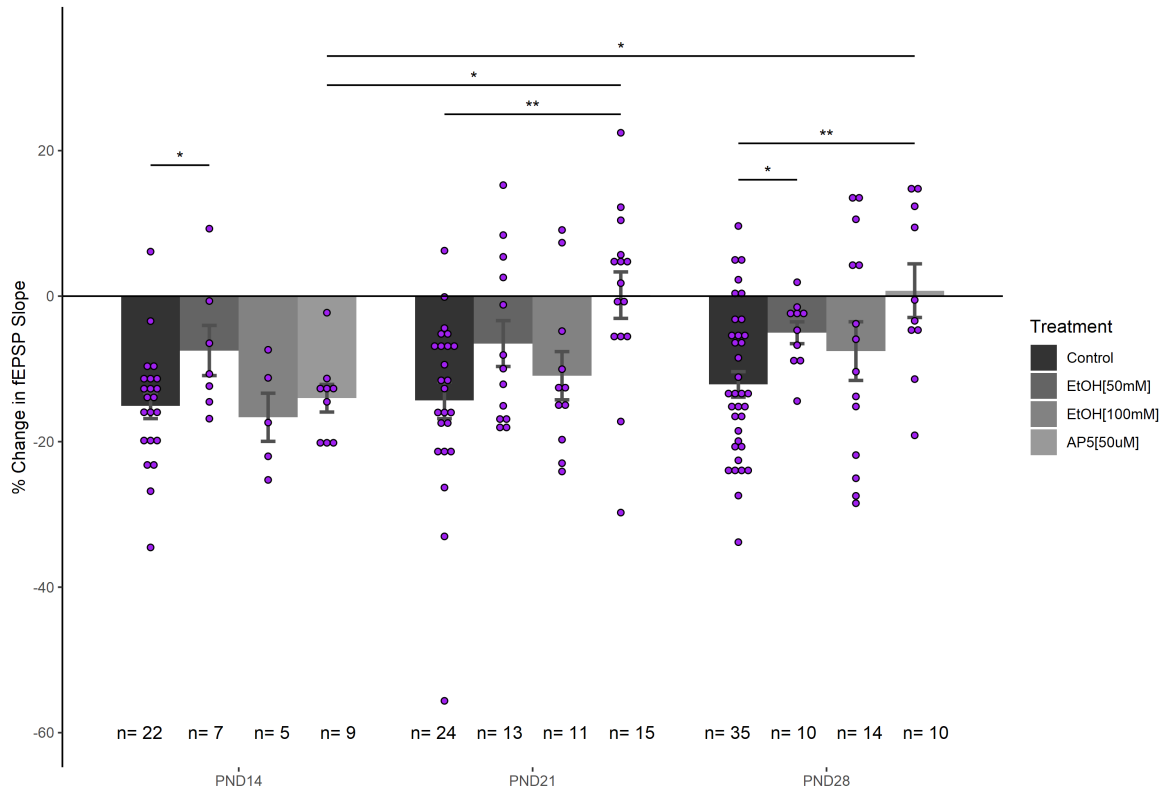


Figure 3.5: Summary figure of significant changes in the effects of NMDAr antagonists to DG-LTD LFS throughout the jDP. Data indicate that significant changes occur in the signaling mechanisms associated with the induction and expression of DG-LTD LFS during DG development.

Table 3.1: Summary of DG-LTD LFS and fEPSP characteristics

Treatment	Slices	Rats	LTD+/-SEM (%)	ExPSP (mV)	Peak Latency (ms)
PND14					
Control	22	12	-15.08 +/- 1.76	-1.08 +/- 0.06	3.41 +/- 0.08
EtOH[50mM]	7	6	-7.47 +/- 3.45	-1.18 +/- 0.1	3.08 +/- 0.09
EtOH[100mM]	5	5	-16.65 +/- 3.31	-0.8 +/- 0.04	3.4 +/- 0.23
AP5[50uM]	9	7	-14.03 +/- 1.9	-1.12 +/- 0.11	3.23 +/- 0.13
PND21					
Control	24	13	-14.31 +/- 2.53	-1.23 +/- 0.09	3.46 +/- 0.08
EtOH[50mM]	13	8	-6.52 +/- 3.15	-1.49 +/- 0.14	3.28 +/- 0.08
EtOH[100mM]	11	4	-10.94 +/- 3.31	-1.16 +/- 0.1	3.39 +/- 0.08
AP5[50uM]	15	7	0.14 +/- 3.19	-1.61 +/- 0.11	3.3 +/- 0.06
PND28					
Control	35	15	-12.14 +/- 1.75	-1.61 +/- 0.15	3.68 +/- 0.09
EtOH[50mM]	10	8	-5.03 +/- 1.5	-1.45 +/- 0.12	3.2 +/- 0.09
EtOH[100mM]	14	6	-7.55 +/- 4.03	-1.3 +/- 0.1	3.37 +/- 0.1
AP5[50uM]	10	5	0.75 +/- 3.69	-1.53 +/- 0.16	3.36 +/- 0.08

Acute 50mM EtOH has developmentally regulated effects on NMDAr-EPSCs

To examine how EtOH affects NMDAr-EPSCs in the developing DG, whole-cell patch clamp was utilized to examine the effects of acute exposure to 50 and 100mM EtOH. Wash in of 50mM EtOH had relatively little effect on NMDAr-EPSCs at PND14 (102.82 +/- 4.13% baseline), a moderate increase in the NMDAr-EPSC at PND21 (113.23 +/- 7.5% of baseline), and a decrease in the magnitude of the NMDAr-EPSC at PND28 (84.2 +/- 7.66 % of baseline) (Figure 3.7). One way ANOVA revealed a significant effect of age on the acute sensitivity of NMDAr-EPSCs to treatment with 50mM EtOH ($F_{(2,26)} = 4.46$, $p = 0.0216$). Follow up analysis revealed significant differences between PND21 and PND28 age groups ($p = 0.016$, TukeyHSD). The normalized change relative to baseline was not significant at any age group (PND14: $p = 0.5$; PND21: $p = 0.109$; PND28: $p = 0.085$; students t-test) .

100mM EtOH trends towards inhibition at each time point

EtOH[100mM] principally resulted in inhibition of the NMDAr EPSC at all three age groups relative to baseline EPSCs (PND14-EtOH[100mM]: 91.93 +/- 7.89%, PND21-EtOH[100mM]: 85.75 +/- 9.18%, PND28-EtOH[100mM]: 81.86 +/- 10.3%) (Figure 3.8). Analysis with one way ANOVA revealed no significant differences between age groups ($F_{(2,18)} = 0.226$, $p = 0.8$). The normalized change relative to baseline was not significant at any age group (PND14: $p = 0.36$; PND21:

$p = 0.16$; PND28: 0.13; student t-test).

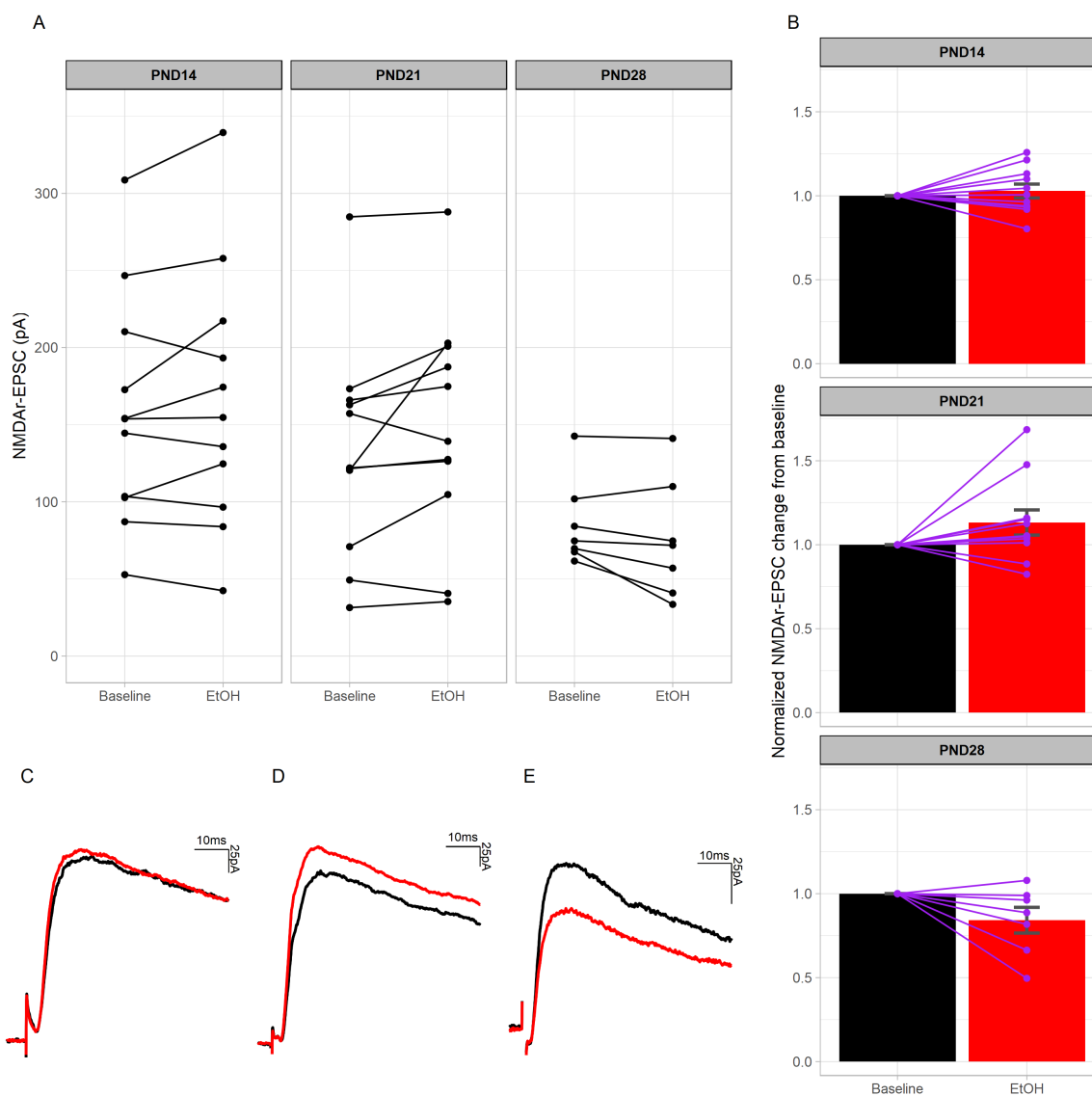


Figure 3.6: NMDAr-EPSCs measured before and after wash in with 50mM EtOH. (A) NMDAr-EPSCs showed no reliable effect at PND14 and PND21, but regularly showed inhibition of the response at PND28. (B) Normalized change relative to baseline for NMDAr-EPSCs at each time point, and the distribution of their responses. (C,D,E) Representative traces of NMDAr-EPSCs before (black) and after (red) EtOH wash in. Responses were taken at +40mV and the NMDAr component was measured 50ms after the onset of the EPSC. Scale bars represent 10ms and 25pA for each example trace.

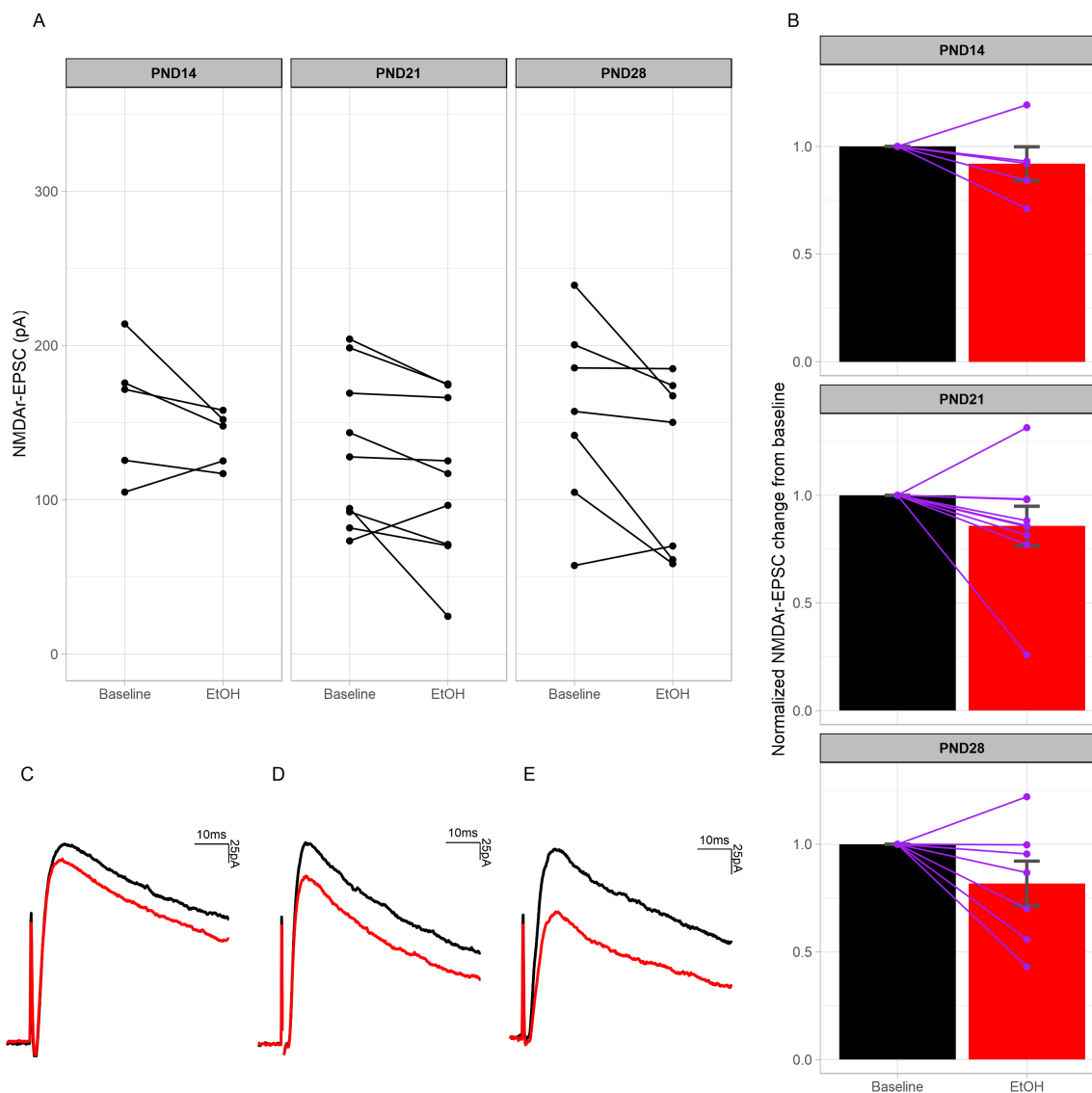


Figure 3.7: NMDAr-EPSCs measured before and after wash in with 100mM EtOH. (A) NMDAr-EPSCs consistently showed inhibition of the response at all three time points. (B) Normalized change relative to baseline for NMDAr-EPSCs at each time point. (C,D,E) Representative traces of NMDAr-EPSCs before (black) and after (red) EtOH wash in. Responses were taken at +40mV and the NMDAr component was measured 50ms after the onset of the EPSC. Scale bars represent 10ms and 25pA for each example trace

CHAPTER 4

Discussion

Summary of results

Data presented here on DG-LTD_{LFS} provide evidence to support significant changes to the signaling mechanisms contributing to DG-LTD_{LFS} throughout the jDP, and describes a developmental role for the NMDAr in DG-LTD_{LFS}. This data also shows moderate attenuation of DG-LTD_{LFS} by EtOH throughout development, and contributes to a relatively small body of literature on the acute effects of EtOH on NMDAr-EPSCs. Three major findings are outlined in this work.

- The first major finding describes the development of a sensitivity of DG-LTD_{LFS} to inhibition of NMDARs by AP5. AP5 significantly inhibited the induction of LTD at PND21 and PND28, but had no significant effect at PND14. Findings observed here regarding the effects of NMDAr inhibition by AP5 on DG-LTD_{LFS} do not directly line up with the other closely related literature (Trommer, Liu, and Pasternak 1996; Wang, Rowan, and Anwyl 1997; Camodeca et al. 1999). Differences are likely related to differences in methodology, including extracellular calcium and magnesium levels, subtle differences in the induction protocol used, subset ages of animals investigated, and inclusion/exclusion criteria for slices reported.
- The second major finding outlined in this work describes developmentally regu-

lated changes in how 50mM EtOH, but not 100mM EtOH, affects DG-LTD_{LFS}. 50mM EtOH attenuated DG-LTD_{LFS} at each time point but only reached statistical significance at PND14 and PND28. At PND28, 50mM EtOH seemed to affect both the magnitude of LTD and the distribution of the response. 100mM EtOH did not have a statistically significant effect on DG-LTD in any age group.

- Finally, the third major finding of this work describes developmentally regulated effects on the acute modulation of NMDAr-EPSCs by 50mM EtOH, that surprisingly does not solely favour inhibition. This novel response of NMDAr-EPSCs to 50mM EtOH is present in the early and mid jDPs, before eventually developing into an acute sensitivity that favours inhibition. In contrast, the effects of 100mM EtOH at all three time points regularly showed inhibition of the NMDAr EPSC.

DG-LTD_{LFS} throughout the jDP

No significant differences in the magnitude of LTD observed at PND14, PND21 and PND28

LFS (900x1Hz) at MPP-DG synapses in the juvenile DG regularly induced a significant decrease in the fEPSP slope at each discrete time point in the jDP (Figure 3.1). Contrary to the literature, data presented here show no significant differences in the magnitude of DG-LTD_{LFS} throughout the jDP, though the probability of inducing LTD decreased with increasing age. Previous reports (Trommer, Liu, and

Pasternak 1996) on DG-LTD_{LFS} in the jDP suggest a decrease in the magnitude of LTD with increasing age, though the authors only include slices in their analysis that achieve a decrease in the fEPSP slope >10%. They report that 100% of slices in the early jDP met their criteria for LTD, while only 70% and 60% of slices in the mid and late time points respectively showed LTD that was >10%.

In the work presented here, 86%, 58% and 86% of slices in the PND14, 21 and 28 groups respectively showed a reduction in synaptic efficacy >10%. The overall magnitude of the DG-LTD_{LFS} observed here is somewhat less than what is generally seen in the literature (Figure 3.1A). Reports on DG-LTD_{LFS} from SD rats of similar ages routinely reported decreases in synaptic efficacy >20% (Trommer, Liu, and Pasternak 1996; Wang, Rowan, and Anwyl 1997; Camodeca et al. 1999). Differences in the magnitude of LTD observed could be related to differences in divalent cations in the perfusion media, subsets of animals involved (age and/or sex), or subtle differences in the induction protocols and analysis methods used between laboratories.

AP5 inhibits DG-LTD_{LFS} at PND21 & PND28, but not PND14

Results presented here show a developmental change in the effects of NMDAR inhibition by AP5 on DG-LTD_{LFS}, occurring between the early and mid to late periods of the jDP (Figure 3.2). Although previous literature seems prominently in favour of NMDAR-independent LTD in the rat DG (Trommer, Liu, and Pasternak 1996; Wang, Rowan, and Anwyl 1997; Camodeca et al. 1999), partial inhibition of LTD is often reported when LFS is applied to MPP synapses in the presence of AP5. Trommer *et al* (Trommer, Liu, and Pasternak 1996) report DG-LTD_{LFS} mea-

suring 76 \pm 10% of baseline that is attenuated to 86 \pm 8% and 87 \pm 4% when LFS was applied in the presence of 20 μ M and 40 μ M AP5 respectively. Similar effects of AP5 are observed by Wang *et al* (Wang, Rowan, and Anwyl 1997), who report DG-LTD_{LFS} measuring 40 \pm 1% of baseline attenuated to 18 \pm 1% when done in the presence of AP5. Another set of experiments done by Camodeca *et al* (Camodeca *et al.* 1999) on 3-5 weeks old SD rats examined whether the Chem-LTD induced by acute application of the group 1 mGluR agonist DHPG occluded further depression of the fEPSP by LFS. In this case authors conclude that LFS after Chem-LTD by DHPG was sufficient to induce further depression of the fEPSP slope that measured 14 \pm 5% and 11 \pm 3% of baseline when done in the presence or absence of PTX respectively. In contrast, when LFS was induced before acute application of DHPG, further depression of the fEPSP was not observed. This indicates that the LFS protocol used to induce DG-LTD was sufficient to induce both the mGluR component of the DG-LTD induced by application of DHPG, as well as any other induction mechanisms potentially influencing the induction and expression of DG-LTD. The magnitude of LTD_{LFS} reported by the authors of this study was 33 \pm 3% (Camodeca *et al.* 1999).

Deciphering the role of NMDARs in DG-LTD_{LFS}

Initial exploration into LTD in the CA1 provided evidence that NMDARs are critical in the induction and expression of LTD_{LFS} (Dudek and Bear 1992; Mulkey and Malenka 1992), but follow up experiments (Oliet, Malenka, and Nicoll 1997) provided strong evidence to support at least two distinct mechanisms contributing to

LTD at hippocampal CA1 synapses. The authors showed one form of LTD reliant on NMDAR signaling and protein phosphatase activity, and another means of inducing LTD that was dependent on mGluR signaling and VGCCs. In both of these cases, sufficient membrane depolarization and an intracellular rise in Ca^{2+} were necessary for inducing LTD, but the origin of the signal could develop through independent mechanisms. What is becoming increasingly clear is that LTD can be induced at individual synapses through a diverse combination of signaling mechanisms dependent on membrane depolarization and a rise in intracellular Ca^{2+} , but the individual contributions of each signaling process and their significant interactions in signaling LTD remains an ongoing field of investigation. While the role for NMDARs in DG-LTD_{LFS} is not entirely clear, there is sufficient evidence to support NMDARs contributing to synapse modification leading to a decrease in synaptic efficacy in the DG (Desmond et al. 1991; Christie and Abraham 1992a; Thiels et al. 1996; Wu et al. 2001; O'Boyle et al. 2004; Yin et al. 2017).

Experiments examining LTD of EPSCs isolated in DGCs of Wistar rats (age 2-3 weeks) performed by Wu et al. (2001) may be one set of experiments able to further elucidate the role of NMDARs in DG-LTD. The authors were able to induce mechanistically distinct forms of DG-LTD that were dependent on activation of either NMDARs or group 1 mGluRs, by pairing post-synaptic depolarizations with HFS of the MPP. Interestingly, the magnitude of the post-synaptic depolarization influenced not only the direction of synaptic plasticity, but also how the presence of AP5 modulated the response (HFS: five trains of eight stimuli at 200 Hz; inter-train interval 200 ms). Post-synaptic depolarizations from -70mV to -30mV lasting

the duration of the HFS protocol (1.1s) induced a potentiation of the EPSC that was converted to a robust depression in the presence of AP5. When the same experiment was done at a holding potential of -50mV, a depression of the synaptic response was observed that was sensitive to inhibition by AP5. Finally, when the post-synaptic depolarization was returned to -70mV for the period between stimulus trains (200ms), no significant effect was observed on the magnitude of the EPSC, even though NMDARs were shown to be moderately activated (Wu et al. 2001).

These results indicate that the level of post-synaptic depolarization reached during LFS may influence whether NMDAR dependent or independent LTD is expressed. It further suggests that release of the Mg^{2+} block and the subsequent NMDAR signaling alongside sufficient mGluR activation are both necessary components in determining the magnitude and/or direction of synaptic change. This further elucidates significant interactions between the NMDAR and the mGluR that may be necessary in governing the direction and/or magnitude of DG-LTD induced after sufficient stimulus.

HFS at MPP-DG synapses *in vivo* in the very young SD rats (PNDs 7-9) also draws on this. O'Boyle et al. (2004) observed different responses to the same stimuli (100 Hz; 1 s; stimulation intensity set to evoke a maximal EPSP) that could be discretely characterized by their post-tetanic response and the long-term (>1 hour) effects on synaptic efficacy (LTP; LTD; STP alone; or STP followed by LTD) (O'Boyle et al. 2004). Much like what was observed by (Wu et al. 2001), an increase in the probability of inducing LTD over LTP was observed when rats were intravenously given the NMDAR antagonist (R,S)-3-(2-carboxy-iperazin-4-yl)propyl-1-phosphonic

acid (CPP). Why the same method of induction has the potential to both increase or decrease synaptic efficacy at MPP-DG synapses, and how developmental time point contributes to this effect is currently unclear.

Changes to NMDAr subunit expression throughout development may affect DG-LTD_{LFS} in the jDP

Developmental changes in the response to LFS could be partially explained by dynamic changes to the NMDAr subunit profile that occurs throughout the jDP (Monyer et al. 1994; Takai et al. 2003). Specific NMDAr subunits have been proposed to regulate the direction of synaptic plasticity (Liu et al. 2004), and different NMDAr expression profiles may affect how mGluR signaling is interpreted at the synapse. Recently published work (O'Neill et al. 2018) has indicated NMDAr modulation by mGluRs in mouse DGCs, adding to a growing body of literature describing interactions between the NMDAr and mGluRs (Rossi, D'Angelo, and Taglietti 1996; Bockaert et al. 2010; Matta et al. 2011).

DG-LTD has also been described in the presynaptic terminals, and can involve both the fast excitatory and inhibitory systems (Chevalleyre and Castillo 2003; Castillo 2012). Novel forms of DG-LTD have also been described involving the EC system and the transient receptor potential (TRPV1) non selective cation channel activated by exogenous capsicum and regulated by endogenous anandamide (Chávez, Chiu, and Castillo 2010). Presynaptic NMDARs have also been proposed to affect synaptic plasticity (Banerjee et al. 2016), but relatively little is known about their role in presynaptic plasticity in the DG.

Conclusions and future directions regarding the role of NMDARs in DG-LTD

This work provides evidence to support significant changes to the mechanisms contributing to the induction and expression of synaptic change after LFS in the DG, characterized by a developmentally regulated change in the sensitivity of DG-LTD_{LFS} to inhibition by AP5 that presents between the early and mid-late juvenile time points. As was previously mentioned, the magnitude of DG-LTD_{LFS} reported here is less than what is regularly reported throughout the literature (Trommer, Liu, and Pasternak 1996; Wang, Rowan, and Anwyl 1997; Camodeca et al. 1999). This discrepancy may elude to differences in the induction protocol used during the conditioning stimulus; in particular, changes to the stimulus intensity or pulse width relative to baseline may influence the expression of LTD *in vitro*. The DG-LTD_{LFS} presented here is done with what could be considered relatively low intensity stimuli, as the stimulation intensity and pulse duration remains unchanged throughout the baseline, condition and decay periods. Adjusting stimulus parameters to maximize the fEPSP response during conditioning stimulus is not unheard of (O'Boyle et al. 2004), and can be observed in the literature by relatively large increases to the fEPSP slope during LFS (Mulkey and Malenka 1992). The LTD_{LFS} outlined here may be insufficient to consistently activate mGluR_{LTD}, yet sufficient enough to signal a NMDAR-dependent component of DG-LTD. Future work to expand upon the results presented here could focus on differentiating between the mGluR and NMDAR dependent components that may be concomitantly activated by LFS.

To investigate this, I would propose experiments to test the hypothesis that in-

creasing the stimulus intensity or pulse duration during the conditioning period has an effect on the magnitude of DG-LTD_{LFS} expressed. Increases in the magnitude of LTD could arise from the recruitment of mGluR dependent mechanisms, along with other potential mechanisms that have been recently described to induce DG-LTD (Chávez, Chiu, and Castillo 2010). I would first approach this question by examining the effects of acute application of DHPG after the low intensity LFS outlined in this work. I hypothesize that, in contrast to Camodeca et al. (1999), acute application of DHPG would induce a further decrease to the fEPSP slope. This would provide evidence to support two discrete but not mutually exclusive signaling processes involved in the induction and expression of DG-LTD. This question could be further expanded upon using whole-cell electrophysiology to further tease apart mechanism underlying the induction and expression of DG-LTD.

Experiments utilizing whole-cell patch clamp could help identify potential interactions between NMDARs and mGluRs in the induction and expression of DG-LTD. The NMDAR is involved in many signaling cascades traditionally thought to be principally dependent on cation flux (review: Luscher and Malenka 2012). AP5 is a competitive antagonist of NMDARs, and recent work has indicated a metabotropic NMDAR signal apparent when NMDAR cation flux is inhibited with the pore blocker MK-801, but not when NMDARs are inhibited by AP5 (Colicos et al. 2016). Using MK-801 to inhibit current flux through NMDARs during DG-LTD, without inhibiting metabotropic coupling of NMDAR activation to other signaling cascades, could potentially unveil signal coupling between NMDARs and mGluR during DG-LTD.

Effects of EtOH on NMDARs and DG-LTD_{LFS}

Developmental time point and concentration are both important factors to consider.

To the best of my knowledge, the acute effects of EtOH on DG-LTD_{LFS} has not been shown. In the CA1, acute EtOH has been reported to both enhance (Hendricson et al. 2002) and inhibit (Izumi et al. 2005) the magnitude of LFS-CA1-LTD in either pooled juvenile (PND12-30) or early adolescent SD rats (PND32-35).

To address this gap in the literature, I investigated the acute effects of EtOH on DG-LTD_{LFS} at each discrete time point to control for the potential that changes to the NMDAR subunit profile may influence the results. The data presented here describes how the expression of DG-LTD_{LFS} is affected by the presence of 50 & 100mM EtOH concentrations (50mM ~ 0.2%BAC) during the conditioning stimulus.

Acute 50mM EtOH exposure resulted in a decrease in the magnitude of DG-LTD_{LFS} for the PND14 and PND28 age groups (Figure 3.3; $p < 0.05$), while almost no effect was observed when the same experiment was done using 100mM EtOH (Figure 3.4 $p > 0.05$ for all ages). The reason behind this inverse effect of concentration on the magnitude of LTD expressed is currently unclear. A close examination of the effects of 50mM EtOH show a surprising change in the relative distribution of LTD_{LFS} expression when comparing PND21 to what was seen at PND28. Going off the work described above on the effects of AP5 (Figure 3.2), and a potential developmental shift in the dominant signaling mechanisms involved in this type of LTD, there remains the possibility that changes to DG-LTD signaling mechanisms during development contributes to differences in the sensitivity of LTD_{LFS} to 50mM and 100mM

EtOH observed between age groups.

EtOH is well characterized as a partial NMDAr antagonist and is proposed to have differential effects on NMDAr comprised of particular subunits. The potential for the acute effects of EtOH on NMDAr to change throughout the jDP led us to investigate how NMDAr-EPSCs are affected at each discrete time point by acute exposure to 50 and 100mM EtOH.

Relatively little work has gone into examining the acute effects of EtOH on NMDAr EPSCs in the DG (Morrisett and Swartzwelder 1993; Ariwodola et al. 2003) compared to the CA1 (Lovinger, White, and Weight 1989; Lahnsteiner and Hermann 1995; Puglia and Valenzuela 2010), and how this changes throughout the jDP has not been investigated. A substantial body of evidence supports EtOH inhibition of NMDAr-EPSCs in a variety of preparations across many brain regions (Hicklin et al. 2011; Wu et al. 2011; Xu et al. 2012; Hughes, Smothers, and Woodward 2013; Zhao et al. 2015).

Surprisingly, 50mM EtOH had relatively little effect on NMDAr-EPSCs at PND14, and regularly showed potentiation of the NMDAr-EPSC at PND21. The effect of EtOH at PND28 was reliably in favour of inhibition, and significant differences were apparent when comparing the PND21 and PND28 group (Figure 3.5; $p < 0.05$). When examining NMDAr-EPSCs after acute exposure to 100mM EtOH, a trend was observed that favoured a moderate decrease in the EPSC at each age group, but the effect was insufficient to reach statistical significance at any time point.

Deciphering the acute effects of EtOH on DG-LTD_{LFS} and NMDAr-EPSCs

Electrophysiological studies have confirmed significant developmental changes to NMDAr subunit expression in DGCs as they mature (Fricke and Prince 1984; Ye et al. 2000; Pedroni et al. 2014). Increases to the ratio of GluN2A:GluN2B subunits is often reported to occur with development (Mameli 2005), alongside relative decreases to the expression of GluN2C and GluN2D subunits. Developmental effects on the response to acute EtOH are well documented within both the excitatory and inhibitory NT systems (Li, Wilson, and Swartzwelder 2002; Mameli 2005; Fleming, Wilson, and Swartzwelder 2007), and this phenomenon is likely in part related to the proposed subunit dependent sensitivity of NMDArs to EtOH (Zhao et al. 2015).

Mameli *et al* show currents isolated in neonatal (PND5) CA3 pyramidal cells responded with potentiated EPSCs to puffs of exogenous NMDA in the presence of 10,20 and 50mM concentrations of EtOH, and a ~15% inhibition in 75mM EtOH (Mameli 2005). Cells obtained in the juvenile CA3 (PND25) responded with dose dependent inhibition that measured up to ~25%. Interestingly though, the potentiation at PND5 was not seen when the excitatory response was delivered by evoking NT release by stimulation of the afferent PP, which synapses onto distal portions of the apical dendritic branches of the CA3 pyramidal cell (Mameli 2005; Witter 2007). The authors eventually conclude a significant presynaptic effect of EtOH on N-type VGCCs at PP-CA3 synapses that inhibits presynaptic glutamate release. How this translates to a potentiated EPSC when puffs of NMDA are used to elicit the excitatory response is not discussed. Whether similar presynaptic effects of EtOH are

present at the MPP-DG synapses, and how this may relate to results presented here will require further investigation. To what degree DG-MPP synapses and CA3-PP synapses share mechanisms for synaptic plasticity is not clear at this time. Results presented here may indicate significant crossover between these two regions as revealed by their unique response to acute to EtOH, but this remains to be seen.

The potentiating effects of EtOH on NMDAR-EPSCs observed in this work may be explained by processes occurring independently of the acute inhibitory effects of EtOH at the receptor. Recent work has indicated EtOH enhancement of neurosteroidogenesis in hippocampal pyramidal neurons by NMDAR activation (Tokuda, Izumi, and Zorumski 2011), and work by Kostakis *et al* (Kostakis et al. 2013) in oocytes has shown evidence for trafficking of NMDARs to the cell surface by signaling processes dependent on the neurosteroid pregnenolone. Whether an effect such as this is present in DG *in vitro* preparations will require further investigation.

EtOH is easily able to permeate the cell membrane, giving it the potential to interfere with intracellular signaling processes, potentially interfering with the signal amplification processes originating at the post-synaptic density during induction (Hicklin et al. 2011; Luscher and Malenka 2012). The two major signaling pathways implemented in LTD involve the PKA and PKC signaling pathways and activation of protein phosphatases (Pöschel and Stanton 2007; Luscher and Malenka 2012). Reports examining the acute effects of EtOH with respect to these pathways have indicated a potential role in PKC signaling (Lahnsteiner and Hermann 1995) and effects that are apparently independent of PKA (Xu and Woodward 2006).

EtOH is also capable of potentiating fast GABAergic signaling (Ariwodola et

al. 2003; Fleming, Wilson, and Swartzwelder 2007), and none of the slices reported here on EtOHs effect on DG-LTD_{LFS} were run in the presence of blockers of GABA_A signaling. The acute effects of EtOH on DG-LTD_{LFS} may have also extend to the GABAergic system and the plasticity expressed there (Chevaleyre and Castillo 2003). Further investigation of the data and the literature is needed.

Conclusions and future directions regarding the acute effects of EtOH on DGCs and DG-LTD_{LFS}

These results indicate a substantial age and concentration dependent effect of EtOH on DG-LTD_{LFS} and NMDAr-EPSCs recorded from DGCs in the developing rat DG, particularly with regards to 50mM EtOH. The acute effects of 50mM EtOH on NMDAr-EPSCs observed at PND14 and PND21 are in stark contrast to what was expected based upon the immediate literature (Morrisett and Swartzwelder 1993; Ariwodola et al. 2003) and what has been observed in other brain regions (Lovinger, White, and Weight 1989; Lahnsteiner and Hermann 1995; Puglia and Valenzuela 2010). While developmental time point and cell type are likely to play a significant role in the divergences observed between this work and the literature, differences in methodology are also important to consider.

A particularly interesting methodological variable is the presence of the redox agents Na-pyruvate and ascorbic acid in the perfusate used for the WC experiments in this work. These compounds are present to reduce the effects of oxidative stress on the cells during the tissue preparation process and throughout the experimental procedure. The NMDAr has been shown to be affected by oxidation and reduction

(Choi, Chen, and Lipton 2001; Bodhinathan, Kumar, and Foster 2010; Talukder, Kazi, and Wollmuth 2011). NMDARs conductance is greater when the protein is in a reduced state, and oxidation of the receptor decreases the ionic conductance. Whether EtOH affects NMDARs differently depending on either the redox state of the local environment, or of the receptor itself, is currently unclear. This could be addressed using whole-cell patch clamp to determine if the sensitivity of NMDAR-EPSCs to EtOH changes with respect to the NMDAR redox state, which could be controlled with redox agents DTT and DTNB (Lipton et al. 1998; Bodhinathan, Kumar, and Foster 2010).

Unfortunately, this potentially confounding variable makes the effects of EtOH on DG-LTD difficult to directly relate to what was observed in DGCs.

A role for mGluR receptors in DG-LTD is well established, and EtOH has been shown to influence LTD_{mGluR} in the cerebellum (De Ruiter et al. 2008; Su, Sun, and Shen 2010). Whether EtOH affects mGluR signaling in this preparation is currently unclear, but could be tested for by examining acute application of DHPG in the presence of EtOH. Considering the potential an increase in the magnitude of LTD along with increasing stimulus intensities during conditioning, further differentiating between types of LTD expressed at MPP-DG synapses may provide insight into the mechanisms of LTD affected by EtOH, and help understand why 50mM but not 100mM EtOH influences the expression of DG-LTD_{LFS} in the jDP.

CHAPTER 5

References

- Abraham, Wickliffe C, Brian R Christie, Barbara Logan, Patricia Lawlor, and M Dragunow. 1994. “Immediate early gene expression associated with the persistence of heterosynaptic long-term depression in the hippocampus.” *Proceedings of the National Academy of Sciences of the United States of America* 91 (21): 10049–53. doi:10.1073/pnas.91.21.10049.
- Acsády, L, A Kamondi, A Sík, Tamás F. Freund, and György Buzsáki. 1998. “GABAergic cells are the major postsynaptic targets of mossy fibers in the rat hippocampus.” *The Journal of Neuroscience : The Official Journal of the Society for Neuroscience* 18 (9): 3386–3403. doi:10.1523/JNEUROSCI.18-09-03386.1998.
- Allaire, J J, Yihui Xie, Jonathan McPherson, Javier Luraschi, Kevin Ushey, Aron Atkins, Hadley Wickham, Joe Cheng, Winston Chang, and Richard Iannone. 2018. *rmarkdown: Dynamic Documents for R*. <https://cran.r-project.org/package=rmarkdown>.
- Amaral, D. G., and M. P. Witter. 1989. “The three-dimensional organization of the hippocampal formation: A review of anatomical data.” *Neuroscience*. doi:10.1016/0306-4522(89)90424-7.
- Amaral, David G, Helen E Scharfman, and Pierre Lavenex. 2007. *The Dentate Gyrus: A Comprehensive Guide to Structure, Function, and Clinical Implications*. Vol. 163. Progress in Brain Research. Elsevier. doi:10.1016/S0079-6123(07)63001-5.
- Aphalo, Pedro J. 2018. *gginnards: Explore the Innards of 'ggplot2' Objects*. <https://cran.r-project.org/package=gginnards>.
- Ariwodola, O J, T L Crowder, K A Grant, J B Daunais, D P Friedman, and J L Weiner. 2003. “Ethanol Modulation of Excitatory and Inhibitory Synaptic Transmission in Rat and Monkey Dentate Granule Neurons.” *Alcoholism: Clinical & Experimental Research* 27 (10): 1632–9. <http://www.ncbi.nlm.nih.gov/pubmed/14574234>.
- Banerjee, Abhishek, Rylan S. Larsen, Benjamin D. Philpot, and Ole Paulsen. 2016. “Roles of Presynaptic NMDA Receptors in Neurotransmission and Plasticity.” *Trends in Neurosciences* 39 (1). Elsevier Ltd: 26–39. doi:10.1016/j.tins.2015.11.001.
- Bates, Douglas, Martin Maechler, Ben Bolker, and Steven Walker. 2019. *lme4: Linear Mixed-Effects Models using 'Eigen' and S4*. <https://cran.r-project.org/>

package=lme4.

- Bayer, Shirley A., and Joseph Altman. 1974. "Hippocampal development in the rat: Cytogenesis and morphogenesis examined with autoradiography and low-level X-irradiation." *Journal of Comparative Neurology* 158 (1): 55–79. doi:10.1002/cne.901580105.
- Beining, Marcel, Tassilo Jungenitz, Tijana Radic, Thomas Deller, Hermann Cuntz, Peter Jedlicka, and Stephan Wolfgang Schwarzacher. 2017. "Adult-born dentate granule cells show a critical period of dendritic reorganization and are distinct from developmentally born cells." *Brain Structure and Function* 222 (3). Springer Berlin Heidelberg: 1427–46. doi:10.1007/s00429-016-1285-y.
- Blaabjerg, Morten, and Jens Zimmer. 2007. "The dentate mossy fibers: structural organization, development and plasticity." *Progress in Brain Research* 163 (07). doi:10.1016/S0079-6123(07)63005-2.
- Bliss, T V, and A R Gardner-Medwin. 1973. "Long-lasting potentiation of synaptic transmission in the dentate area of the unanaesthetized rabbit following stimulation of the perforant path." *The Journal of Physiology* 232 (2): 357–74. <http://www.ncbi.nlm.nih.gov/pubmed/4727085>
<http://www.pubmedcentral.nih.gov/articlerender.fcgi?artid=PMC1350459>.
- Bockaert, Joël, Paul Worley, Federica Bertaso, Laurent Fagni, Fabrice Ango, and Gautier Roussignol. 2010. "Homer1a-Dependent Crosstalk Between NMDA and Metabotropic Glutamate Receptors in Mouse Neurons." *PLoS ONE* 5 (3): e9755. doi:10.1371/journal.pone.0009755.
- Bodhinathan, Karthik, Ashok Kumar, and Thomas C. Foster. 2010. "Intracellular Redox State Alters NMDA Receptor Response during Aging through Ca²⁺/Calmodulin-Dependent Protein Kinase II." *Journal of Neuroscience* 30 (5): 1914–24. doi:10.1523/JNEUROSCI.5485-09.2010.
- Cajal, Santiago Ramónc; n Y Ramon Y. 1894. "The Croonian Lecture: La Fine Structure des Centres Nerveux." *Proceedings of the Royal Society of London* 55 (331-335). The Royal Society: 444–68. doi:10.1098/rspl.1894.0063.
- Camodeca, Nicoletta, Nicholas A. Breakwell, Michael J. Rowan, and Roger Anwyl. 1999. "Induction of LTD by activation of group I mGluR in the dentate gyrus in vitro." *Neuropharmacology* 38 (10): 1597–1606. doi:10.1016/S0028-3908(99)00093-3.
- Carnevale, Nicholas T, K Y Tsai, B J Claiborne, and T H Brown. 1997. "Comparative electrotonic analysis of three classes of rat hippocampal neurons." *Journal of Neurophysiology* 78 (2): 703–20. doi:10.1080/10810730.2014.914606.
- Castillo, Pablo E. 2012. "Presynaptic LTP and LTD of excitatory and inhibitory synapses." *Cold Spring Harbor Perspectives in Biology* 4 (2). doi:10.1101/cshperspect.a005728.
- Castillo, Pablo E., Thomas J. Younts, Andrés E. Chávez, and Yuki Hashimoto-dani.

2012. “Endocannabinoid Signaling and Synaptic Function.” *Neuron* 76 (1): 70–81. doi:10.1016/j.neuron.2012.09.020.
- Chandrasekar, Raman. 2013. “Alcohol and NMDA receptor: current research and future direction.” *Frontiers in Molecular Neuroscience* 6 (May): 14. doi:10.3389/fnmol.2013.00014.
- Chávez, Andrés E., Chiayu Q. Chiu, and Pablo E. Castillo. 2010. “TRPV1 activation by endogenous anandamide triggers postsynaptic long-term depression in dentate gyrus.” *Nature Neuroscience* 13 (12): 1511–8. doi:10.1038/nn.2684.
- Chevaleyre, Vivien, and Pablo E. Castillo. 2003. “Heterosynaptic LTD of hippocampal GABAergic synapses: A novel role of endocannabinoids in regulating excitability.” *Neuron* 38 (3): 461–72. doi:10.1016/S0896-6273(03)00235-6.
- Choi, Y, H V Chen, and S a Lipton. 2001. “Three pairs of cysteine residues mediate both redox and zn²⁺ modulation of the nmda receptor.” *The Journal of Neuroscience : The Official Journal of the Society for Neuroscience* 21 (2): 392–400. doi:21/2/392 [pii].
- Christie, Brian R, and Wickliffe C Abraham. 1992a. “NMDA-dependent heterosynaptic long-term depression in the dentate gyrus of anaesthetized rats.” *Synapse* 10 (1): 1–6. doi:doi:10.1002/syn.890100102.
- Christie, Brian R., and Wickliffe C. Abraham. 1992b. “Priming of associative long-term depression in the dentate gyrus by θ frequency synaptic activity.” *Neuron* 9 (1): 79–84. doi:10.1016/0896-6273(92)90222-Y.
- Colicos, Michael A, Travis Rilea, Jennifer Bialecki, Valentyna Maslieieva, Ian R Winship, Evelyn M M Ma, Nathan T Ikuta, et al. 2016. “Metabotropic NMDA receptor signaling couples Src family kinases to pannexin-1 during excitotoxicity.” *Nature Neuroscience* 19 (3): 432–42. doi:10.1038/nn.4236.
- Collingridge, Graham L., Stephane Peineau, John G. Howland, and Yu Tian Wang. 2010. “Long-term depression in the CNS.” *Nature Reviews Neuroscience* 11 (7): 459–73. doi:10.1038/nrn2867.
- Coultrap, Steven J., Ronald K. Freund, Heather O’Leary, Jennifer L. Sanderson, Katherine W. Roche, Mark L. Dell’Acqua, and K. Ulrich Bayer. 2014. “Autonomous CaMKII mediates both LTP and LTD using a mechanism for differential substrate site selection.” *Cell Reports* 6 (3). The Authors: 431–37. doi:10.1016/j.celrep.2014.01.005.
- Coultrap, Steven J., Kristin M. Nixon, Rachel M. Alvestad, C. Fernando Valenzuela, and Michael D. Browning. 2005. “Differential expression of NMDA receptor subunits and splice variants among the CA1, CA3 and dentate gyrus of the adult rat.” *Molecular Brain Research* 135 (1-2): 104–11. doi:10.1016/j.molbrainres.2004.12.005.
- Cummings, Jennifer a., Rosel M. Mulkey, Roger a. Nicoll, and Robert C. Malenka. 1996. “Ca²⁺ signaling requirements for long-term depression in the hippocam-

- pus." *Neuron* 16 (4): 825–33. doi:10.1016/S0896-6273(00)80102-6.
- De Ruiter, Martijn, Christian Hansel, C. Fernando Valenzuela, Chris I. De Zeeuw, Amor Belmeguenai, Mario Carta, Paolo Botta, and John T. Weber. 2008. "Alcohol Impairs Long-Term Depression at the Cerebellar Parallel Fiber–Purkinje Cell Synapse." *Journal of Neurophysiology* 100 (6): 3167–74. doi:10.1152/jn.90384.2008.
- Debanne, Dominique, and Scott M. Thompson. 1996. "Associative long-term depression in the hippocampus in vitro." *Hippocampus* 6 (1): 9–16. doi:10.1002/(SICI)1098-1063(1996)6:1<9::AID-HIPO3>3.0.CO;2-M.
- Desmond, Nancy L., Costa M. Colbert, De Xing Zhang, and William B. Levy. 1991. "NMDA receptor antagonists block the induction of long-term depression in the hippocampal dentate gyrus of the anesthetized rat." *Brain Research* 552 (1): 93–98. doi:10.1016/0006-8993(91)90664-H.
- Dowle, Matt, and Arun Srinivasan. 2019. *data.table: Extension of 'data.frame'*. <https://cran.r-project.org/package=data.table>.
- Dudek, S M, and M F Bear. 1992. "Homosynaptic long-term depression in area CA1 of hippocampus and effects of N-methyl-D-aspartate receptor blockade." *Proceedings of the National Academy of Sciences of the United States of America* 89 (10): 4363–7. doi:10.1073/pnas.89.10.4363.
- Dunwiddie, T., and G. Lynch. 1978. "Long-term potentiation and depression of synaptic responses in the rat hippocampus: localization and frequency dependency." *The Journal of Physiology* 276 (1): 353–67. doi:10.1113/jphysiol.1978.sp012239.
- Erreger, Kevin, Shashank M. Dravid, Tue G. Banke, David J A Wyllie, and Stephen F. Traynelis. 2005. "Subunit-specific gating controls rat NR1/NR2A and NR1/NR2B NMDA channel kinetics and synaptic signalling profiles." *Journal of Physiology* 563 (2): 345–58. doi:10.1113/jphysiol.2004.080028.
- Felthouser, Alicia M., and Brenda J. Claiborne. 1990. "Intracellular labeling of dentate granule cells in fixed tissue permits quantitative analysis of dendritic morphology." *Neuroscience Letters* 118 (2): 249–51. doi:10.1016/0304-3940(90)90639-Q.
- Fleming, Rebekah L, Wilkie A Wilson, and H Scott Swartzwelder. 2007. "Magnitude and ethanol sensitivity of tonic GABAA receptor-mediated inhibition in dentate gyrus changes from adolescence to adulthood." *Journal of Neurophysiology* 97 (5): 3806–11. doi:10.1152/jn.00101.2007.
- Fricke, R. A., and D. A. Prince. 1984. "Electrophysiology of dentate gyrus granule cells." *Journal of Neurophysiology* 51 (2): 195–209. doi:10.1152/jn.1984.51.2.195.
- Galindo, Rafael, Paula A. Zamudio, and C. Fernando Valenzuela. 2005. "Alcohol is a potent stimulant of immature neuronal networks: Implications for fetal alcohol spectrum disorder." *Journal of Neurochemistry* 94 (6): 1500–1511.

doi:10.1111/j.1471-4159.2005.03294.x.

- Gonçalves, J. Tiago, Simon T. Schafer, and Fred H. Gage. 2016. “Adult Neurogenesis in the Hippocampus: From Stem Cells to Behavior.” *Cell* 167 (4): 897–914. doi:10.1016/j.cell.2016.10.021.
- Hafting, Torkel, Marianne Fyhn, Sturla Molden, May Britt Moser, and Edvard I. Moser. 2005. “Microstructure of a spatial map in the entorhinal cortex.” *Nature* 436 (7052): 801–6. doi:10.1038/nature03721.
- Hansen, Kasper B., Kevin K. Ogden, Hongjie Yuan, and Stephen F. Traynelis. 2014. “Distinct functional and pharmacological properties of triheteromeric GluN1/GluN2A/GluN2B NMDA receptors.” *Neuron* 81 (5): 1084–96. doi:10.1016/j.neuron.2014.01.035.
- Harney, S. C., M Rowan, and R Anwyl. 2006. “Long-Term Depression of NMDA Receptor-Mediated Synaptic Transmission Is Dependent on Activation of Metabotropic Glutamate Receptors and Is Altered to Long-Term Potentiation by Low Intracellular Calcium Buffering.” *Journal of Neuroscience* 26 (4): 1128–32. doi:10.1523/JNEUROSCI.2753-05.2006.
- Hendricson, Adam W, C L Alek Miao, Melanie J Lippmann, and Richard a Morrisett. 2002. “Ifenprodil and ethanol enhance NMDA receptor-dependent long-term depression.” *The Journal of Pharmacology and Experimental Therapeutics* 301 (3): 938–44. doi:10.1124/jpet.301.3.938.
- Henson, Maile A., Charles J. Tucker, Meilan Zhao, and Serena M. Dudek. 2016. “Long-term depression-associated signaling is required for an in vitro model of NMDA receptor-dependent synapse pruning.” *Neurobiology of Learning and Memory* 138: 39–53. doi:10.1016/j.nlm.2016.10.013.
- Hicklin, Tianna R, Peter H Wu, Richard A Radcliffe, Ronald K Freund, Susan M Goebel-Goody, Paulo R Correa, William R Proctor, Paul J Lombroso, and Michael D Browning. 2011. “Alcohol inhibition of the NMDA receptor function, long-term potentiation, and fear learning requires striatal-enriched protein tyrosine phosphatase.” *Proceedings of the National Academy of Sciences of the United States of America* 108 (16): 6650–5. doi:10.1073/pnas.1017856108.
- Higley, Michael J, and Bernardo L Sabatini. 2012. “Calcium signaling in dendritic spines.” *Cold Spring Harbor Perspectives in Biology* 4 (4): a005686. doi:10.1101/cshperspect.a005686.
- Hobbiss, Anna F, Yazmin Ramiro Cortes, and Inbal Israely. 2018. “Homeostatic plasticity scales dendritic spine volumes and changes the threshold and specificity of Hebbian plasticity.” *bioRxiv*, 308965. doi:10.1101/308965.
- Hodgkin, A. L., and A. F. Huxley. 1945. “Resting and action potentials in single nerve fibres.” *The Journal of Physiology* 104 (2): 176–95. <http://www.ncbi.nlm.nih.gov/pubmed/16991677>.
- Hughes, Benjamin A., C. Thetford Smothers, and John J. Woodward. 2013. “De-

- phosphorylation of GluN2B C-terminal tyrosine residues does not contribute to acute ethanol inhibition of recombinant NMDA receptors.” *Alcohol* 47 (3). Elsevier Ltd: 181–86. doi:10.1016/j.alcohol.2012.12.015.
- Hulme, Sarah R., Owen D. Jones, Clarke R. Raymond, Pankaj Sah, and Wickliffe C. Abraham. 2014. “Mechanisms of heterosynaptic metaplasticity.” *Philosophical Transactions of the Royal Society B: Biological Sciences* 369 (1633). doi:10.1098/rstb.2013.0148.
- Izumi, Y., K. Nagashima, K. Murayama, and C. F. Zorumski. 2005. “Acute effects of ethanol on hippocampal long-term potentiation and long-term depression are mediated by different mechanisms.” *Neuroscience* 136 (2): 509–17. doi:10.1016/j.neuroscience.2005.08.002.
- Jaffe, David B., and Rafael Gutiérrez. 2007. “Mossy fiber synaptic transmission: communication from the dentate gyrus to area CA3.” *Progress in Brain Research* 163. doi:10.1016/S0079-6123(07)63006-4.
- Jones, Shawn P., Omid Rahimi, Michael P. O’Boyle, Daniel L. Diaz, and Brenda J. Claiborne. 2003. “Maturation of granule cell dendrites after mossy fiber arrival in hippocampal field CA3.” *Hippocampus* 13 (3): 413–27. doi:10.1002/hipo.10121.
- Kandel, Eric R., and W Alden Spencer. 1968. “Cellular neurophysiological approaches in the study of learning.” *Physiological Reviews* 48 (1): 65–134. doi:10.1152/physrev.1968.48.1.65.
- Kesner, Raymond P. 2018. “An analysis of dentate gyrus function (an update).” *Behavioural Brain Research* 354 (February 2017). Elsevier: 84–91. doi:10.1016/j.bbr.2017.07.033.
- Kostakis, Emmanuel, Conor Smith, Ming-Kuei Jang, Stella C Martin, Kyle G Richards, Shelley J Russek, Terrell T Gibbs, and David H Farb. 2013. “The neuroactive steroid pregnenolone sulfate stimulates trafficking of functional N-methyl D-aspartate receptors to the cell surface via a noncanonical, G protein, and Ca²⁺-dependent mechanism.” *Molecular Pharmacology* 84 (2): 261–74. doi:10.1124/mol.113.085696.
- Lahnsteiner, E., and A. Hermann. 1995. “Acute action of ethanol on rat hippocampal CA1 neurons: effects on intracellular signaling.” *Neuroscience Letters* 191 (3): 153–56. doi:10.1016/0304-3940(95)11579-L.
- Lawrence, J. Josh, Zachary M. Grinspan, and Chris J. McBain. 2004. “Quantal transmission at mossy fibre targets in the CA3 region of the rat hippocampus.” *Journal of Physiology* 554 (1): 175–93. doi:10.1113/jphysiol.2003.049551.
- Li, Qiang, WA Wilson, and HS Swartzwelder. 2002. “Differential effect of ethanol on NMDA EPSCs in pyramidal cells in the posterior cingulate cortex of juvenile and adult rats.” *Journal of Neurophysiology* 87: 705–11. <http://jn.physiology>.

org/content/87/2/705.short.

- Lima-Landman, Maria Teresa R, and Edson X. Albuquerque. 1989. “Ethanol potentiates and blocks NMDA-activated single-channel currents in rat hippocampal pyramidal cells.” *FEBS Letters* 247 (1): 61–67. doi:10.1016/0014-5793(89)81241-4.
- Lipton, S a, P V Rayudu, Y B Choi, N J Sucher, and H S Chen. 1998. “Redox modulation of the NMDA receptor by NO-related species.” *Progress in Brain Research* 118: 73–82. doi:10.1007/PL00000638.
- Lisman, John. 2017. “Glutamatergic synapses are structurally and biochemically complex because of multiple plasticity processes: long-term potentiation, long-term depression, short-term potentiation and scaling.” *Philosophical Transactions of the Royal Society B: Biological Sciences* 372 (1715): 20160260. doi:10.1098/rstb.2016.0260.
- Liu, Lidong, T P Wong, M F Pozza, K Lingenhoehl, Y T Wang, M Sheng, Y P Auber-son, and Y T Wang. 2004. “Role of NMDA receptor subtypes in governing the direction of hippocampal synaptic plasticity.” *Science* 304 (5673): 1021–4. doi:10.1126/science.1096615\n304/5673/1021 [pii].
- Liu, X, Shilpa Tilwalli, G Ye, Peter A. Lio, Joseph F. Pasternak, and Barbara L. Trommer. 2000. “Morphologic and electrophysiologic maturation in developing dentate gyrus granule cells.” *Brain Research* 856 (1-2): 202–12. doi:10.1016/S0006-8993(99)02421-X.
- Lovinger, David M, Geoffrey White, and Forrest F Weight. 1989. “Ethanol Inhibits NMDA-Activated Ion Current in Hippocampal Neurons” 243 (4899): 1721–4.
- Lovinger, David M., and Karina P. Abrahao. 2018. “Synaptic plasticity mechanisms common to learning and alcohol use disorder.” *Learning and Memory* 25 (9): 425–34. doi:10.1101/lm.046722.117.
- Luscher, Christian, and Robert C Malenka. 2012. “NMDA Receptor-Dependent Long-Term Potentiation and Long-Term Depression (LTP / LTD).” *Cold Spring Harbor Perspectives in Biology* 4: 1–16.
- Lynch, G, R.L. Smith, P. Mensah, and C. Cotman. 1973. “Tracing the Dentate Gyrus Mossy Fiber System Peroxidase Histochemistry with Horseradish.” *Experimental Neurology* 524: 516–24.
- Mameli, M. 2005. “Developmentally Regulated Actions of Alcohol on Hippocampal Glutamatergic Transmission.” *Journal of Neuroscience* 25 (35): 8027–36. doi:10.1523/JNEUROSCI.2434-05.2005.
- Matta, Jose A., Michael C. Ashby, Antonio Sanz-Clemente, Katherine W. Roche, and John T.R. Isaac. 2011. “MGluR5 and NMDA Receptors Drive the Experience- and Activity-Dependent NMDA Receptor NR2B to NR2A Subunit Switch.” *Neuron* 70 (2). Elsevier Inc.: 339–51. doi:10.1016/j.neuron.2011.02.045.
- Medvedev, N. I., V. I. Popov, J. J. Rodriguez Arellano, G. Dallérac, H. A. Davies,

- P. L. Gabbott, S. Laroche, I. V. Kraev, V. Doyère, and M. G. Stewart. 2010. “The N-methyl-d-aspartate receptor antagonist CPP alters synapse and spine structure and impairs long-term potentiation and long-term depression induced morphological plasticity in dentate gyrus of the awake rat.” *Neuroscience* 165 (4). Elsevier Inc.: 1170–81. doi:10.1016/j.neuroscience.2009.11.047.
- Mezey, Szilvia, Valérie Doyère, Ian De Souza, Elaine Harrison, Karine Cambon, Claire E. Kendal, Heather Davies, Serge Laroche, and Michael G. Stewart. 2004. “Long-term synaptic morphometry changes after induction of long-term potentiation and long-term depression in the dentate gyrus of awake rats are not simply mirror phenomena.” *European Journal of Neuroscience* 19 (8): 2310–8. doi:10.1111/j.0953-816X.2004.03334.x.
- Milner, Austen J, Damian M Cummings, Jonathan P Spencer, and Kerry P S J Murphy. 2004. “Bi-directional plasticity and age-dependent long-term depression at mouse CA3-CA1 hippocampal synapses.” *Neuroscience Letters* 367 (1): 1–5. doi:10.1016/j.neulet.2004.04.056.
- Monyer, Hannah, Nail Burnashev, David J. Laurie, Bert Sakmann, and Peter H. Seeburg. 1994. “Developmental and regional expression in the rat brain and functional properties of four NMDA receptors.” *Neuron* 12 (3): 529–40. doi:10.1016/0896-6273(94)90210-0.
- Morrisett, RA, and HS Swartzwelder. 1993. “Attenuation of hippocampal long-term potentiation by ethanol: a patch-clamp analysis of glutamatergic and GABAergic mechanisms.” *J. Neurosci.* 13 (5): 2264–72. <http://www.jneurosci.org/content/13/5/2264.short>.
- Mu, Yangling, Chunmei Zhao, Nicolas Toni, Jun Yao, and Fred H. Gage. 2015. “Distinct roles of NMDA receptors at different stages of granule cell development in the adult brain.” *eLife* 4 (OCTOBER2015): 1–18. doi:10.7554/eLife.07871.
- Mulkey, Rosel M., and Robert C. Malenka. 1992. “Mechanisms underlying induction of homosynaptic long-term depression in area CA1 of the hippocampus.” *Neuron* 9 (5): 967–75. doi:10.1016/0896-6273(92)90248-C.
- Muñoz, Pablo, Genaro C. Barrientos, Gina Sánchez, Cecilia Hidalgo, Alejandra Arias-Cavieres, and Claudio Elgueta. 2018. “Ryanodine Receptor-Mediated Calcium Release Has a Key Role in Hippocampal LTD Induction.” *Frontiers in Cellular Neuroscience* 12 (November): 1–12. doi:10.3389/fncel.2018.00403.
- Münster-Wandowski, Agnieszka, Gisela Gómez-Lira, and Rafael Gutiérrez. 2013. “Mixed neurotransmission in the hippocampal mossy fibers.” *Frontiers in Cellular Neuroscience* 7 (November): 1–19. doi:10.3389/fncel.2013.00210.
- Nagy, Jozsef. 2004. “The NR2B subtype of NMDA receptor: a potential target for the treatment of alcohol dependence.” *Current Drug Targets. CNS and Neurological Disorders* 3 (3): 169–79.
- Navarrete, Marta, and Alfonso Araque. 2010. “Endocannabinoids potentiate synaptic

- transmission through stimulation of astrocytes.” *Neuron* 68 (1). Elsevier Inc.: 113–26. doi:10.1016/j.neuron.2010.08.043.
- Oliet, Stéphane H.R., Robert C. Malenka, and Roger A. Nicoll. 1997. “Two distinct forms of long-term depression coexist in CA1 hippocampal pyramidal cells.” *Neuron* 18 (6): 969–82. doi:10.1016/S0896-6273(00)80336-0.
- O’Boyle, Michael P., Viet Do, Brian E. Derrick, and Brenda J. Claiborne. 2004. “In Vivo Recordings of Long-Term Potentiation and Long-Term Depression in the Dentate Gyrus of the Neonatal Rat.” *Journal of Neurophysiology* 91 (2): 613–22. doi:10.1152/jn.00307.2003.
- O’Mara, S M, M J Rowan, and R Anwyl. 1995. “Dantrolene inhibits long-term depression and depotentiation of synaptic transmission in the rat dentate gyrus.” *Neuroscience* 68 (3): 621–4. <http://www.ncbi.nlm.nih.gov/pubmed/8577362>.
- O’Mara, S. M., M. J. Rowan, and R. Anwyl. 1995. “Metabotropic glutamate receptor-induced homosynaptic long-term depression and depotentiation in the dentate gyrus of the rat hippocampus in vitro.” *Neuropharmacology* 34 (8): 983–89. doi:10.1016/0028-3908(95)00062-B.
- O’Neill, Nathanael, Catherine McLaughlin, Noboru Komiyama, and Sergiy Sylantsev. 2018. “Biphasic modulation of NMDA receptor function by metabotropic glutamate receptors.” *The Journal of Neuroscience* 38 (46): 1000–1018. doi:10.1523/JNEUROSCI.1000-18.2018.
- Paoletti, Pierre, Camilla Bellone, and Qiang Zhou. 2013. “NMDA receptor subunit diversity: impact on receptor properties, synaptic plasticity and disease.” *Nature Reviews. Neuroscience* 14 (6). Nature Publishing Group: 383–400. doi:10.1038/nrn3504.
- Pedroni, Andrea, Do Duc Minh, Antonello Mallamaci, and Enrico Cherubini. 2014. “Electrophysiological characterization of granule cells in the dentate gyrus immediately after birth.” *Frontiers in Cellular Neuroscience* 8 (February): 1–9. doi:10.3389/fncel.2014.00044.
- Peoples, R W, G White, D M Lovinger, and F F Weight. 1997. “Ethanol inhibition of N-methyl-D-aspartate-activated current in mouse hippocampal neurones: whole-cell patch-clamp analysis.” *Br J Pharmacol* 122 (6): 1035–42. doi:10.1038/sj.bjp.0701483.
- Pinar, Cristina, Christine J. Fontaine, Juan Triviño-Paredes, Carina P. Lottenberg, Joana Gil-Mohapel, and Brian R. Christie. 2017. “Revisiting the flip side: Long-term depression of synaptic efficacy in the hippocampus.” *Neuroscience and Biobehavioral Reviews* 80 (June): 394–413. doi:10.1016/j.neubiorev.2017.06.001.
- Piña-Crespo, Juan C, and Alasdair J Gibb. 2002. “Subtypes of NMDA receptors in new-born rat hippocampal granule cells.” *The Journal of Physiology* 541 (Pt 1):

- 41–64. doi:10.1113/jphysiol.2001.014001.
- Pöschel, Beatrice, and Patric K. Stanton. 2007. “Comparison of cellular mechanisms of long-term depression of synaptic strength at perforant path-granule cell and Schaffer collateral-CA1 synapses.” *Progress in Brain Research* 163: 473–500. doi:10.1016/S0079-6123(07)63026-X.
- Puglia, Michael P., and C. Fernando Valenzuela. 2010. “Ethanol acutely inhibits ionotropic glutamate receptor-mediated responses and long-term potentiation in the developing CA1 hippocampus.” *Alcoholism, Clinical and Experimental Research* 34 (4): 594–606. doi:10.1111/j.1530-0277.2009.01128.x.
- R Core Team. 2018. *R: A Language and Environment for Statistical Computing*. Vienna, Austria: R Foundation for Statistical Computing. <https://www.r-project.org/>.
- Rahimi, Omid, and Brenda J. Claiborne. 2007. “Morphological development and maturation of granule neuron dendrites in the rat dentate gyrus.” In *Progress in Brain Research*, r:167–81. doi:10.1016/S0079-6123(07)63010-6.
- Ren, Hong, Yulin Zhao, Donard S. Dwyer, and Robert W. Peoples. 2012. “Interactions among positions in the third and fourth membrane-associated domains at the intersubunit interface of the N-Methyl-D-aspartate receptor forming sites of alcohol action.” *Journal of Biological Chemistry* 287 (33): 27302–12. doi:10.1074/jbc.M111.338921.
- Rihn, Laura L., and Brenda J. Claiborne. 1990. “Dendritic growth and regression in rat dentate granule cells during late postnatal development.” *Developmental Brain Research* 54 (1): 115–24. doi:10.1016/0165-3806(90)90071-6.
- Rollenhagen, A., K. Satzler, E. P. Rodriguez, P. Jonas, M. Frotscher, and J. H. R. Lübke. 2007. “Structural Determinants of Transmission at Large Hippocampal Mossy Fiber Synapses.” *Journal of Neuroscience* 27 (39): 10434–44. doi:10.1523/JNEUROSCI.1946-07.2007.
- Rossi, Paola, Egidio D’Angelo, and Vanni Taglietti. 1996. “Differential Long-lasting Potentiation of the NMDA and Non-NMDA Synaptic Currents Induced by Metabotropic and NMDA Receptor Coactivation in Cerebellar Granule Cells.” *European Journal of Neuroscience* 8 (6): 1182–9. doi:10.1111/j.1460-9568.1996.tb01286.x.
- Scoville, WB, and B. Milner. 1957. “Loss of recent memory after bilateral hippocampal lesions.” *Journal of Neurology, Neurosurgery, and Psychiatry* 20 (1): 11–21. doi:10.1136/jnnp.20.1.11.
- Seress, L, and J Pokorny. 1981. “Structure of the granular layer of the rat dentate gyrus. A light microscopic and Golgi study.” *Journal of Anatomy* 133 (Pt 2): 181–95.
- Shatz, Carla J. 1992. “The developing brain.” *Scientific American* 267 (3): 60–67.

- doi:10.1038/scientificamerican0992-60.
- Squire, L., and S Zola-Morgan. 1991. "The medial temporal lobe memory system." *Science* 253 (5026): 1380–6. doi:10.1126/science.1896849.
- Squire, Larry R. 2009. "The Legacy of Patient H.M. for Neuroscience." *Neuron* 61 (1): 6–9. doi:10.1016/j.neuron.2008.12.023.
- Staubli, Ursula V., and Zhan Xin Ji. 1996. "The induction of homo- vs. heterosynaptic LTD in area CA1 of hippocampal slices from adult rats." *Brain Research* 714 (1-2): 169–76. doi:10.1016/0006-8993(95)01523-X.
- Stephens, Jeremy, Kirill Simonov, Yihui Xie, Zhuoer Dong, Hadley Wickham, Jeffrey Horner, Reikoch, Will Beasley, Brendan O'Connor, and Gregory R Warnes. 2018. *yaml: Methods to Convert R Data to YAML and Back*. <https://cran.r-project.org/package=yaml>.
- Su, Li Da, Cheng Long Sun, and Ying Shen. 2010. "Ethanol acutely modulates mGluR1-Dependent long-term depression in cerebellum." *Alcoholism: Clinical and Experimental Research* 34 (7): 1140–5. doi:10.1111/j.1530-0277.2010.01190.x.
- Suvarna, Yashasvi, Nivedita Maity, and M. C. Shivamurthy. 2016. "Emerging Trends in Retrograde Signaling." *Molecular Neurobiology* 53 (4): 2572–8. doi:10.1007/s12035-015-9280-5.
- Takai, Hirotake, Kei-ichi Katayama, Koji Uetsuka, Hiroyuki Nakayama, and Kunio Doi. 2003. "Distribution of N-methyl-d-aspartate receptors (NMDARs) in the developing rat brain." *Experimental and Molecular Pathology* 75 (1). Academic Press: 89–94. doi:10.1016/S0014-4800(03)00030-3.
- Talukder, Iehab, Rashek Kazi, and Lonnie P. Wollmuth. 2011. "GluN1-specific redox effects on the kinetic mechanism of NMDA receptor activation." *Biophysical Journal* 101 (10). Biophysical Society: 2389–98. doi:10.1016/j.bpj.2011.10.015.
- Thiels, Edda, Xiaping Xie, Mark F. Yeckel, German Barrionuevo, and Theodore W. Berger. 1996. "NMDA receptor-dependent LTD in different subfields of hippocampus in vivo and in vitro." *Hippocampus* 6 (1): 43–51. doi:10.1002/(SICI)1098-1063(1996)6:1<43::AID-HIPO8>3.0.CO;2-8.
- Tokuda, K., Y. Izumi, and C. F. Zorumski. 2011. "Ethanol Enhances Neurosteroidogenesis in Hippocampal Pyramidal Neurons by Paradoxical NMDA Receptor Activation." *Journal of Neuroscience* 31 (27): 9905–9. doi:10.1523/jneurosci.1660-11.2011.
- Tokuda, K., C. F. Zorumski, and Y. Izumi. 2007. "Modulation of hippocampal long-term potentiation by slow increases in ethanol concentration." *Neuroscience* 146 (1): 34–49. doi:10.1016/j.neuroscience.2007.01.037.
- Trommer, Barbara L., Ying Bing Liu, and Joseph F. Pasternak. 1996. "Long-term depression at the medial perforant path-granule cell synapse in developing rat dentate gyrus." *Developmental Brain Research* 96 (1-2): 97–108.

doi:10.1016/0165-3806(96)00104-6.

- Urbanek, Simon. 2013. *png: Read and write PNG images*. <https://cran.r-project.org/package=png>.
- Vicini, Stefano, J F Wang, Jin Hong Li, Wei Jian Zhu, Yue Hua Wang, Jian Hong Luo, Barry B. Wolfe, and Dennis R. Grayson. 1998. “Functional and pharmacological differences between recombinant N-methyl-D-aspartate receptors.” *Journal of Neurophysiology* 79 (2): 555–66. doi:10.1152/jn.1998.79.2.555.
- Wang, Y, M J Rowan, and R Anwyl. 1997. “Induction of LTD in the dentate gyrus in vitro is NMDA receptor independent, but dependent on Ca²⁺ influx via low-voltage-activated Ca²⁺ channels and release of Ca²⁺ from intracellular stores.” *Journal of Neurophysiology* 77 (2): 812–25. <http://jn.physiology.org/content/77/2/812.abstract>.
- Wang, Zhuo, Dong Song, and Theodore W. Berger. 2002. “Contribution of NMDA receptor channels to the expression of LTP in the hippocampal dentate gyrus.” *Hippocampus* 12 (5): 680–88. doi:10.1002/hipo.10104.
- Wenzel, Andreas, Jean Marc Fritschy, Hanns Mohler, and Dietmar Benke. 1997. “NMDA Receptor Heterogeneity During Postnatal Development of the Rat Brain: Differential Expression of the NR2A, NR2B, and NR2C Subunit Proteins.” *Journal of Neurochemistry* 68 (2): 469–78. doi:10.1046/j.1471-4159.1997.68020469.x.
- White, Collin C, Hannah Viernes, Cecile M Krejsa, Dianne Botta, and Terrence J Kavanagh. 2003. “Fluorescence-based microtiter plate assay for glutamate–cysteine ligase activity.” *Analytical Biochemistry* 318 (2): 175–80. doi:10.1016/S0003-2697(03)00143-X.
- Wickham, Hadley. 2016. *ggplot2: Elegant Graphics for Data Analysis*. Springer-Verlag New York. <http://ggplot2.org>.
- . 2017. *tidyverse: Easily Install and Load the 'Tidyverse'*. <https://cran.r-project.org/package=tidyverse>.
- Wickham, Hadley, and Jennifer Bryan. 2018. *usethis: Automate Package and Project Setup*. <https://cran.r-project.org/package=usethis>.
- Wickham, Hadley, Peter Danenberg, and Manuel Eugster. 2018. *roxygen2: In-Line Documentation for R*. <https://cran.r-project.org/package=roxygen2>.
- Wilkerson, Julia R., Joseph P. Albanesi, and Kimberly M. Huber. 2018. “Roles for Arc in metabotropic glutamate receptor-dependent LTD and synapse elimination: Implications in health and disease.” *Seminars in Cell and Developmental Biology* 77. Elsevier Ltd: 51–62. doi:10.1016/j.semcd.2017.09.035.
- Wills, T. A., T. L. Kash, and D. G. Winder. 2013. “Developmental changes in the acute ethanol sensitivity of glutamatergic and GABAergic transmission in the

- BNST.” *Alcohol* 47 (7). Elsevier Ltd: 531–37. doi:10.1016/j.alcohol.2013.08.003.
- Wirkner, K, W Poelchen, L Köles, K Mühlberg, P Scheibler, C Allgaier, and P Illes. 1999. “Ethanol-induced inhibition of NMDA receptor channels.” *Neurochemistry International* 35 (2). Pergamon: 153–62. doi:10.1016/S0197-0186(99)00057-1.
- Witter, Menno P. 2007. “The perforant path: projections from the entorhinal cortex to the dentate gyrus.” *Progress in Brain Research* 163: 43–61. doi:10.1016/S0079-6123(07)63003-9.
- Wright, J M, R W Peoples, and F F Weight. 1996. “Single-channel and whole-cell analysis of ethanol inhibition of NMDA-activated currents in cultured mouse cortical and hippocampal neurons.” *Brain Research* 738 (2): 249–56. doi:10.1016/S0006-8993(96)00780-9.
- Wu, Jinqian, Anthony Rush, Michael J. Rowan, and Roger Anwyl. 2001. “NMDA receptor- and metabotropic glutamate receptor-dependent synaptic plasticity induced by high frequency stimulation in the rat dentate gyrus in vitro.” *Journal of Physiology* 533 (3): 745–55. doi:10.1111/j.1469-7793.2001.t01-1-00745.x.
- Wu, Peter H, Steven J Coultrap, Michael D Browning, and William R Proctor. 2011. “Functional Adaptation of the N-Methyl- D -aspartate Receptor to Inhibition by Ethanol Is Modulated by Striatal-Enriched Protein Tyrosine Phosphatase and p38 Mitogen-Activated Protein Kinase.” *Molecular Pharmacology* 80 (3): 529–37. doi:10.1124/mol.110.068643.NMDAR.
- Xie, Yihui. 2018. *knitr: A General-Purpose Package for Dynamic Report Generation in R*. <https://cran.r-project.org/package=knitr>.
- Xu, Minfu, and John J. Woodward. 2006. “Ethanol inhibition of NMDA receptors under conditions of altered protein kinase A activity.” *Journal of Neurochemistry* 96 (6): 1760–7. doi:10.1111/j.1471-4159.2006.03703.x.
- Xu, Minfu, C Thetford Smothers, James Trudell, and John J Woodward. 2012. “Ethanol inhibition of constitutively open N-methyl-D-aspartate receptors.” *The Journal of Pharmacology and Experimental Therapeutics* 340 (1): 218–26. doi:10.1124/jpet.111.187179.
- Ye, Gui Lan, Xue Song Liu, Joseph F. Pasternak, and Barbara L. Trommer. 2000. “Maturation of glutamatergic neurotransmission in dentate gyrus granule cells.” *Developmental Brain Research* 124 (1-2): 33–42. doi:10.1016/S0165-3806(00)00103-6.
- Yin, Pengcheng, Hao Xu, Qi Wang, Jiayue Wang, Liang Yin, Meichen Xu, Zhenyang Xie, Wenzhao Liu, and Xiaohua Cao. 2017. “Overexpression of β CaMKII impairs behavioral flexibility and NMDAR-dependent long-term depression in the dentate gyrus.” *Neuropharmacology* 116. Elsevier Ltd: 270–87. doi:10.1016/j.neuropharm.2016.12.013.
- Zhao, Yulin, Hong Ren, Donard S. Dwyer, and Robert W. Peoples. 2015. “Different

sites of alcohol action in the NMDA receptor GluN2A and GluN2B subunits.”
Neuropharmacology 97. Elsevier Ltd: 240–50. doi:10.1016/j.neuropharm.2015.05.018.

Zhu, Hao. 2019. *kableExtra: Construct Complex Table with 'kable' and Pipe Syntax*.
<https://cran.r-project.org/package=kableExtra>.

Zorumski, Charles F., Steven Mennerick, and Yukitoshi Izumi. 2014. “Acute
and chronic effects of ethanol on learning-related synaptic plasticity.” *Alcohol*
(Fayetteville, N.Y.) 48 (1). Elsevier Ltd: 1–17. doi:10.1016/j.alcohol.2013.09.045.